Redox Biology 28 (2020) 101365

Contents lists available at ScienceDirect

Redox Biology

journal homepage: www.elsevier.com/locate/redox

Succinate accumulation induces mitochondrial reactive oxygen species generation and promotes status epilepticus in the kainic acid rat model

Yurong Zhang[a,1], Mengdi Zhang[a,1], Wei Zhu[b], Jie Yu[a], Qiaoyun Wang[a], Jinjin Zhang[a], Yaru Cui[a], Xiaohong Pan[a], Xue Gao[a], Hongliu Sun[a,*]

[a] School of Pharmaceutical Sciences, Binzhou Medical University, Yantai, 264003, China
[b] Institute of Radiation Medicine, Shandong Academy of Medical Sciences, Jinan, 250062, China

ARTICLE INFO

Keywords:
Status epilepticus
Succinate
Reactive oxygen species
Neurodegeneration
Mitophagy

ABSTRACT

Though succinate accumulation is associated with reactive oxygen species (ROS) production and neuronal injury, which play critical roles in epilepsy, it is unclear whether succinate accumulation contributes to the onset of epilepsy or seizures. We sought to investigate changes in succinate, oxidative stress, and mito-SOX levels, as well as mitophagy and neuronal change, in different status epilepticus (SE) rat models. Our results demonstrate that KA-induced SE was accompanied by increased levels of succinate, oxidative stress, and mito-SOX, as well as mitophagy and neuronal degeneration. The similarly increased levels of succinate, oxidative stress, and mito-SOX were also found in pilocarpine-induced SE. Moreover, the reduction of succinate accumulation by the inhibition of succinate dehydrogenase (SDH), malate/aspartate shuttle (MAS), or purine nucleotide cycle (PNC) served to reduce succinate, oxidative stress, and mito-SOX levels, thereby preventing oxidative stress-related neuronal damage and lessening seizure severity. Interestingly, simulating succinate accumulation with succinic acid dimethyl ester may induce succinate accumulation and increased oxidative stress and mito-SOX levels, as well as behavior and seizures in electroencephalograms similar to those observed in rats exposed to KA. Our results indicate that succinate accumulation may contribute to the increased oxidative stress/mitochondrial ROS levels, neuronal degeneration, and SE induced by KA administration. Furthermore, we found that succinate accumulation was mainly due to the inverse catalysis of SDH from fumarate, which was supplemented by the MAS and PNC pathways. These results reveal new insights into the mechanisms underlying SE and that reducing succinate accumulation may be a clinically useful therapeutic target in SE.

1. Introduction

Epilepsy is the second most common disease of the nervous system, affecting approximately 0.5-1% of the population worldwide, with greater drug resistance and worse clinical outcomes than many other neurological diseases [1]. The poor outcome is closely associated with unclear and complex pathogenesis of epilepsy. Given this, it is critical to study the mechanisms underlying epilepsy to facilitate the development of novel antiepileptic targets.

Recent studies have suggested that reactive oxygen species (ROS), and especially mitochondrial ROS (mito-ROS), contribute to neuronal damage in seizures or epilepsy and play a vital role in disease pathogenesis [2–4]. For example, a common animal model of epilepsy that involves the systemic administration of kainic acid (KA) causes oxidative stress, evidenced by ROS production in the rat brain and mitochondrial dysfunction [5,6]. Moreover, increased mitochondrial oxidative stress and dysfunction were found in animal models of temporal lobe epilepsy (TLE), such as kainic acid (KA), pilocarpine, and pentylenetetrazole (PTZ) treatment models [7].

The production of ROS/mitochondrial ROS is associated with

Abbreviations: (AOA), Aminooxyacetate acid; (AICAR), 5-aminoimidazole-4-carboxamide-1-b-D-ribofuranoside; (AP), anteroposterior; (DM), dimethylmalonate; (DMSO), dimethyl sulfoxide; (DV), dorsoventral; (EEGs), electroencephalograms; (ETC), electron transport chain; (FJB), fluoro-jade B; (GSD), generalized seizure duration; (KA), kainic acid; (MAS), malate/aspartate shuttle; (ML), mediolateral; (PTZ), pentylenetetrazole; (PNC), purine nucleotide cycle; (ROS), reactive oxygen species; (RET), reverse electron transport; (SE), status epilepticus; (SDH), succinate dehydrogenase; (SAD), succinic acid dimethyl ester; (TLE), temporal lobe epilepsy; (TOMM20), translocase of outer mitochondrial outer membrane 20

* Corresponding author.
E-mail address: sun_china6@163.com (H. Sun).
[1] These authors contributed equally to this work.

https://doi.org/10.1016/j.redox.2019.101365
Received 19 September 2019; Received in revised form 15 October 2019; Accepted 28 October 2019
Available online 31 October 2019

defects of mitochondria. For example, the production of ROS may be partly due to a defect in mitochondria [8] that leads to altered energy consumption and energy dyshomeostasis. This critical mechanism may underlie epilepsy [9,10]. In addition, oxidative stress affects additional metabolic processes and might contribute to neuronal excitability and the development of epilepsy [11]. Moreover, mitochondrial ROS production-induced metabolic impairments also play a vital role in epileptogenesis and occur in a widespread manner with the development of epilepsy [12].

Alternatively, the accumulation of damaged mitochondria in the brain may result from increased mitochondrial ROS [13,14]. There are many sources of mitochondrial ROS, including complex I (NADH dehydrogenase), complex II (succinate dehydrogenase, SDH), and complex III (coenzyme Q-cytochrome C reductase) of the electron transport chain (ETC) [15]. Related studies have also indicated that the ROS signaling may be mainly derived from reverse electron transport (RET) to the ETC at complex I [16]. Inhibition of complex I of the ETC induces mitochondrial ROS, oxidative damage, and increased neuronal loss [17].

The mechanism underlying RET at complex I is a topic of critical importance. One suspected possibility is that succinate generates ROS by driving RET at complex I [18,19]. The role of succinate accumulation in mitochondrial ROS production and neuronal damage has attracted significant attention in recent years [20–22]. Succinate is at a cross-road between several metabolic pathways and plays an important role in them, functioning to collect pools of catabolic molecules and initiating anabolic processes [23].

The fumarate-malate-oxaloacetate pathway, initiated by succinate, is potentially the most critical metabolic cycle [24]. In this pathway, SDH (complex II) serves as a key enzyme responsible for oxidizing succinate to fumarate and maintaining ROS homeostasis in mitochondria through the production and elimination of superoxide [23]. However, previous studies [18,20] suggest that in ischemia/reperfusion animal model, during ischemia, succinate accumulates due to the reverse catalysis of SDH. Subsequent re-oxidization of accumulated succinate by SDH, thus, generates excess mitochondrial ROS. This re-oxidization of accumulated succinate results in the further generation of ROS via reverse electron flow through complex I [25]. Based on the effect of succinate on ROS generation and production by driving RET at complex I [18] and the importance of ROS in epilepsy, we speculate that increased ROS caused by succinate accumulation may be involved in the pathological changes seen in epilepsy, although the role of succinate in epilepsy is less clear.

Normally, to circumvent the citric acid cycle, succinate is catalyzed by SDH to fumarate [26]. If succinate accumulates from fumarate with the reverse catalysis of SDH in epilepsy, the source(s) of fumarate must be identified. There are two critical pathways as sources of fumarate: the malate/aspartate shuttle (MAS), wherein a high NADH/NAD^+ ratio (complex I) drives malate formation which then gets converted to fumarate, and the purine nucleotide cycle (PNC) [27–30]. These pathways have been confirmed to contribute to succinate accumulation under the reverse catalysis of SDH in pathological conditions [18]. Given this and prior evidence, we predict that succinate accumulation may underlie neuronal injury and seizures in epilepsy. More specifically, SDH reversal from fumarate, which is sourced from the MAS and PNC pathways, may be the main source of succinate accumulation.

Given this background, we sought to investigate the changes of succinate level during KA-induced status epilepticus (SE) in rats and further explore the possible source of excessive succinate. Furthermore, we evaluated the effects of inhibiting succinate accumulation via different pathways and those of simulating succinate accumulation on seizure and neuronal injury to explore the role of succinate accumulation.

2. Material and methods

2.1. Animals

Male Sprague-Dawley rats (280-300g, No. SCXK2014-0006, provided by Jifeng Experimental Animal Center; 210-230g, No. SCXK2019-0003, provided by Pengyue Experimental Animal Center; Jinan, China) were used in our experiments. All experiments abided by the National Institutes of Health Guide for the Care and Use of Laboratory Animals (NIH Publications No. 80-23, revised 1996) requirements. According to the guiding principles of the Binzhou Medical University Animal Experimentation Committee, which approved the study (approval no. 2016002), animals were singly housed. Water and food were provided *ad libitum*. All experiments were carried out between 8:00 and 17:00.

2.2. Surgery and KA-induced SE

As previously described [31], after administering anesthetic (sodium pentobarbital, 50 mg/kg, i.p.; CAS, 57-33-0, Xiya Reagent, China), rats (280-300g) were head-fixed using a stereotaxic apparatus. Then, 3-cm-long stainless steel electrodes with a diameter of 0.2 mm each (0.5 mm of the insulating layer removed from their tips; A.M. Systems, USA) were implanted into the right cortex (anteroposterior, AP: 3.2 mm; mediolateral, ML: 3.0 mm; dorsoventral, DV: 1.8 mm) for electroencephalogram (EEG) recording. A stainless-steel cannula (RSD Life Science, China) was implanted into the left lateral ventricle (AP: 1.8 mm, ML: 1 mm, DV: 3.6 mm). The implanted electrodes and cannula were fixed to the skull using dental cement. Five days after surgery, rats were injected with kainic acid (KA, 1 mg/0.8 mL, 0.65 μL/rat, CAS, 58002-62-3, Sigma-Aldrich, USA) into the left lateral ventricles. Animals were then placed into a Plexiglas arena (50 cm × 30 cm × 30 cm) and their behavior and EEGs (AD Instruments, Sydney, NSW, Australia) were recorded for 60 min. Seizure severity was classified as stage 1–5 [32]. Stages one through three featured focal seizures, while stages four and five featured generalized seizures.

2.3. Pilocarpine-induced SE

Briefly, male Sprague-Dawley rats (210-230g) were injected with lithium chloride (127 mg/kg, i.p.; CAS, 7447-41-8, Ruijinte, China) 20 h before pilocarpine administration. Bromomethyl scopolamine (1 mg/kg, i.p.; CAS, 155-41-9, Sigma, USA) was administered 20 min before a single intraperitoneal injection of pilocarpine hydrochloride (30 mg/kg, i.p.; CAS, 54-71-7, Sigma, USA) to attenuate the peripheral muscarinic effects. After pilocarpine treatment, the rats were observed for the development of continuous seizure activity. SE was allowed to continue for 90 min until diazepam (2 mg/kg, i.p.; CAS, 439-14-5, Sigma, USA) was injected to terminate seizure activity.

2.4. Pharmacological manipulations

In our study, generalized seizures in most rats appeared immediately following KA administration and were terminated with diazepam (1 mg/mL solution at a dose of 0.002 mg/g body weight i.p.; CAS, 439-14-5, Sigma-Aldrich, USA) 60 min after KA administration. Aminooxyacetate acid (AOA, 31.25 μg/5 μL in saline, CAS, 15R0027H, J&W Pharmlab, Shanghai, China), a specific inhibitor of the MAS, or saline were injected into the lateral ventricles 30 min before KA treatment in KA + AOA/saline group. In 5-Aminoimidazole-4-carboxamide-1-b-D-ribofuranoside (AICAR)-treated group (KA + AICAR), AICAR (1.5 μg/5 μL in dimethyl sulfoxide [DMSO], CAS, 01177254, Acros, Belgium) was injected into the left lateral ventricles 60 min before KA treatment, and the control group was treated with DMSO (KA + DMSO). Lateral ventricle injections were performed with a needle (RSD Life Science, China) that matched the cannula planted into the left lateral ventricles, with the tip of the needle inserted 0.2 mm

below the guide cannula. The injection took 10 min, and after the injection, the needle was left in place for 2 min before being slowly retracted. Dimethylmalonate (DM, 1 mL/kg [1.15 g/mL] dissolved in ethanol, then in saline; CAS, 136441-250G, Sigma-Aldrich, USA), an SDH competitive inhibitor, or saline were injected (i.p.) 15 min before KA treatment (KA + DM/saline group). AOA, AICAR, and DM were injected daily for 3 days. Succinic acid dimethyl ester (SAD, 100 μg/2 μL in DMSO, CAS, 106-60-0, Damas-beta, Shanghai, China) and DMSO were injected continuously into the left lateral ventricle for 30 min. The details of pharmacological manipulations are shown in Supplementary Fig. 1.

2.5. Succinate accumulation

Four rats per time point (5 min, 30 min, 24 h, and 3 days) after KA or pilocarpine treatment from each group, respectively, were anesthetized and then, rapidly decapitated before their brains were removed. We dissected the hippocampus and cortex out of each brain for succinate colorimetric assessments (MAK184, Sigma-Aldrich, USA). A 1 mM (1 nmol/μL) succinate standard solution was then prepared, and standards for colorimetric detection (0, 2, 4, 6, 8, and 10 μL of 1 mM succinate standard solution) were plated into a 96-well plate, generating 0 (blank), 2, 4, 6, 8, and 10 nmol/well standards. Succinate assay buffer was then added to each well to bring the total volume up to 50 μL. Sample tissue (10 mg) was then rapidly added to 100 μL of ice-cold succinate assay buffer and centrifuged at 10,000 g for 5 min to remove any precipitate from the supernatant, which was retained. Next, 50 μL of the appropriate reaction mix was added to each reaction well. These were incubated for 30 min at 37 °C and protected from light. Absorbance was then measured using a bicinchoninic acid assay kit (MAK184, Sigma-Aldrich, USA) at 450 nm.

2.6. Measurement of oxidative stress

Oxidative stress measurements were performed on the dissected hippocampi and cortices of four rats from each group sacrificed at four time points (5 min, 30 min, 24 h, and 3 days) after KA or pilocarpine treatment respectively (S0033, Beyotime Institute of Biotechnology, China). We dissected out the hippocampus and cortex. These different regions were soaked separately in cell staining buffer (0.01 M phosphate-buffered saline [PBS], Shanghai Novland Co., Ltd., China). Filtration was used to prepare a single-cell suspension, which was incubated with a ROS marker, 2′,7′-dichlorofluorescin diacetate (DCF-DA, S0033, Beyotime Institute of Biotechnology, China) at 37 °C for 60 min. Tissues were then washed three times with PBS. A fluorescence microplate reader (Thermo, USA) was used to measure excitation at 488 nm and emission at 525 nm.

2.7. Mitochondrial ROS assessment by fluorescence and flow cytometry

After KA or pilocarpine treatment, the rats from each group were sacrificed at four time points (5 min, 30 min, 24 h, and 3 days) under anesthesia before their brains were rapidly removed. We dissected out the hippocampus and cortex to measure regional mitochondrial ROS using the Mito-SOX reagent (M36008, Thermo Fisher, USA). Each region was soaked separately in cell staining buffer. Filtration was used to prepare a single cell suspension. As per previous reports [33], a 5 μM Mito-SOX working solution was then prepared. Next, 1.0 mL of the 5 μM Mito-SOX reagent was applied as a cell loading solution in which cells were incubated for 10 min at 37 °C without light exposure. Cells were then gently washed three times with warm PBS. Excitation wavelengths were measured at 510 nm and emission at 580 nm by a fluorescence microplate reader (Thermo, USA) and flow cytometer (Becton, Dickinson and Company, USA).

2.8. Immunohistochemistry

As described previously [34,35], 24 h and 3 days after KA administration, we used sodium pentobarbital (50 mg/kg, i.p.) to deeply anesthetize five rats per timepoint from each group. We opened the chest and exposed the heart to rapidly inject 250 mL of saline and then 250 mL of 4% paraformaldehyde fixation solution into the left ventricle. The rats were beheaded and brains were removed and post-fixed for at least 24 h in 4% paraformaldehyde before being transferred into 30% sucrose until they sank. We then prepared 10-μm-thick brain sections with a cryostat microtome (CM3050s, Leica, Germany).

LC3B/TOMM20/DAPI immunofluorescent staining was then performed. Brain sections were washed for 15 min with PBS and then with 10% bovine serum albumin in PBS to block non-specific binding for 2 h at room temperature. After blocking, sections were incubated in primary antibody dilution buffer, which contained a mixture of mouse anti-TOMM20 (1:100; ab56783, Abcam, UK) and rabbit anti-LC3B (1:100; ab48394, Abcam, UK) at 4 °C overnight. Sections were washed three times in PBS and then incubated in a secondary antibody dilution buffer containing a mixture of Cy3-conjugated (1:200; Beyotime Institute of Biotechnology, Jiangsu, China) and fluorescein isothiocyanate-conjugated (1:200, EMD Millipore, USA) secondary antibodies. While on a shaking table, sections were washed three times in PBS for 15 min each and then incubated in 4′,6-diamidino-2-phenylindole (C1005, Beyotime, China) for 15 min at room temperature. Lastly, all sections were washed three times with PBS on the shaking table and then cover-slipped.

A laser confocal microscope (LSM880, Zeiss, Germany) was used to assess hippocampal and cortical LC3B/TOMM20/DAPI expression after different interventions. At the same brightness level, fluorescence intensities were compared between regions. As previously described [34,35], Image J V.1.37 software (National Institutes of Health, Bethesda, MD) was used to analyze the fluorescence intensities.

2.9. Fluoro-Jade B (FJB) staining

FJB (AG310-30MG; EMD Millipore, USA), a polyanionic fluorescein derivative, which sensitively and specifically binds to degenerating neurons [36,37], was used to label tissues at two timepoints (24 h and 3 days after KA administration). As above, five rats per timepoint per group were deeply anesthetized and perfused intracardially with normal saline and then 4% paraformaldehyde. Coronal 10-μm-thick slices were made using a cryostat (CM3050s, Leica, Germany). Tissues were first immersed in 80% alcohol solution containing 1% sodium for 5 min. Next, they were soaked in 70% alcohol for 2 min and then in distilled water for 2 min. To ensure equivalent background between slides, all slides were immersed in a 0.06% potassium permanganate solution for 15 min on a shaking table and then rinsed for 2 min with distilled water. Dye powder was used to make a 0.01% FJB stock solution that was stored at 4 °C. Next, 100 mL of staining solution was made with 96 mL of 0.1% acetic acid vehicle and 4 mL of FJB stock solution. All slides were then soaked in the staining solution for 20 min and then rinsed for 1 min with distilled water. After 1 min of rinsing, slides were placed in an oven set to 50 °C for 5 min. Finally, the dry slides were immersed in xylene for at least 1 min. All slides were mounted with neutral balsam and then imaged by using an epifluorescent microscope with blue (450 nm) excitation light (Carl Zeiss AG, Germany). The number of positive signals was counted manually.

2.10. Western blotting

As previously described [1], after KA administration for 24 h or 3 days, four rats per group were decapitated and their brains were rapidly removed. We dissected out the hippocampus and the cortex and extracted protein from each. To measure protein concentrations with a bicinchoninic acid assay kit (P0012, Beyotime Institute of

Biotechnology, China), all proteins were loaded with a loading buffer. We used 10% sodium dodecyl sulfate polyacrylamide gels to separate proteins, and then, electrophoresis and electroblotting on a polyvinylidene difluoride membrane were performed. The membrane was then blocked for 3h with 5% fat-free milk at room temperature and incubated with rabbit monoclonal LC3B (1:1,000; ab48394, Abcam, UK) or glyceraldehyde-3-phosphate dehydrogenase (GAPDH; 1:3,000; AB-P-R001, Zhejiang Kangcheng Biotech, Hangzhou, China) overnight at 4 °C on a shaking table. Horseradish peroxidase-conjugated IgG was used as a secondary antibody and slides were incubated with this for 2 h at room temperature. All images were acquired and analyzed with the Odyssey infrared imaging system (LI-COR Biosciences, USA). Results are expressed as ratios relative to GAPDH expression.

2.11. Electron microscopy

Four rats from each group were anesthetized and perfused as described in the Immunohistochemistry section and the brains were microdissected to isolate the hippocampal dentate gyrus (DG), CA3, and entorhinal cortex (EC). These subregions were placed on ice. The dissected subregions were fixed with 2.0% glutaraldehyde for 24 h, washed three times, and postfixed with 1% osmic acid for 2 h. The subregions were dehydrated with an acetone series and propylene oxide at 4 °C, then embedded in resin. Ultrathin sections were cut and doubly stained with lead citrate and uranyl acetate. Data were acquired by transmission electron microscopy (ZEISS, Germany).

2.12. Statistical analyses

Values are presented as means ± SEMs. SPSS 13.0 (SPSS Inc., USA) was used to perform all statistical analyses. The nonparametric Mann-Whitney *U* test was used to analyze the cumulative time spent at each seizure stage as well as changes in succinate, DCF, and mito-SOX levels and the expression of proteins. Comparisons of the seizure duration and generalized seizure duration (GSD) were made via one-way ANOVA. For all analyses, $P < 0.05$ was considered to be statistically significant.

3. Results

3.1. Increased succinate, DCF, and mito-SOX levels in KA- or policarpine-induced SE

In the KA group (n = 84), KA was administrated directly to the lateral ventricle to explore resultant changes in succinate accumulation and DCF, and mito-SOX levels. Animals in the control group (n = 84) were administrated equal doses of saline. From 5 min onwards, succinate levels became significantly higher than those in the control group (hippocampus, $P = 0.002$, Fig. 1A; cortex, $P = 0.003$, Fig. S2A). Similar increases in DCF levels also occurred (hippocampus, $P < 0.001$, Fig. 1B; cortex, $P < 0.001$, Fig. S2B). Levels of hippocampal and cortical mito-SOX signal were also elevated after KA treatment ($P < 0.001$, Fig. 1C, Fig. S2C). A similar increase in succinate, DCF, and mito-SOX levels was also found in pilocarpine-induced SE (n = 72; hippocampus, Fig. 1D–F; cortex, Figs. S2D–F) compared with controls treated with saline (n = 72). The severity of rat seizures was evaluated by accumulated GSD and seizure duration. We found that rats in the KA group spent significantly more time in stages four and five than did saline control animals (stage 4: 27.8 ± 1.2 min *vs.* 0 min; stage 5: 26.8 ± 1.3 min *vs.* 0 min; $P < 0.001$ for both, Fig. 1I). Cumulative GSD was 54.6 ± 0.3 min, while seizure duration was 56.8 ± 0.2 min (Fig. 1G and H). No generalized seizures or seizure-like discharge were identified in control rats treated with saline instead of KA (Fig. 1G–I). Representative EEGs and their power spectra are shown in Fig. 1K.

3.2. Increased mitophagy and neuronal degeneration in KA-induced SE

We performed additional experiments to investigate changes in mitophagy and neuronal degeneration (n = 60). LC3B can induce mitophagy and is used to assess mitophagy [38]. We evaluated changes in LC3B via immunohistochemistry and western blots (Fig. 2A–G) and found that mitophagy was significantly increased in the hippocampus ($P < 0.001$, Fig. 2A–G) as well as in the cortex ($P < 0.001$, Fig. 2E–G).

Neuronal degeneration is often evaluated via FJB staining [36,37]. Our results revealed obvious FJB signal increases in the hippocampus in the KA group relative to controls ($P < 0.001$, Fig. 2H-M). Transmission electron microscopy analysis revealed similar neuronal injury (Fig. 2N and O). These results indicate that consistent with the succinate accumulations and increased oxidative stress, mitophagy and neuronal degeneration were also increased with KA treatment.

3.3. DM, an SDH competitive inhibitor, reversed increased succinate/oxidative stress, and attenuated KA-induced SE

DM is rapidly hydrolyzed to produce cellular malonate and is used as an effective competitive inhibitor of SDH oxidation [22]. In rats treated with DM (KA + DM group, n = 56), we found that the increased succinate and DCF levels induced by KA were reversed more (in both the hippocampus and the cortex) with DM treatment from the first timepoint (5 min) than in saline-treated controls (hippocampal succinate: $P < 0.001$; cortical succinate: $P = 0.002$; hippocampal DCF: $P = 0.045$; cortical DCF: $P = 0.016$; Fig. 3A–D). Increased mito-SOX levels in the hippocampus and cortex, which occurred synchronously after KA administration were also reversed in the KA + DM group (hippocampal: $P = 0.002$; cortical: $P = 0.043$; Fig. 3E and F). Similar changes in the levels of hippocampal and cortical mito-SOX signal after DM treatment in KA-induced SE were found using flow cytometry (Fig. 3J). Moreover, animal behavior and EEG results indicated that DM-treated animals spent less time in stage 5 ($P < 0.001$; 42.5 ± 1.3 min *vs.* 16.1 ± 0.5 min; Fig. 3G) and more time in stages 0–3 ($P < 0.001$; 5.1 ± 0.7 min *vs.* 17.9 ± 0.8 min; Fig. 3G) and stage 4 ($P < 0.001$; 12.4 min ± 0.8 *vs.* 26.0 ± 1.0 min; Fig. 3G). Meanwhile, decreased GSD ($P < 0.001$; 54.9 ± 0.7 min *vs.* 42.1 ± 0.8 min; Fig. 3H) and seizure duration ($P < 0.001$; 57.1 ± 0.5 min *vs.* 47.4 ± 0.7 min; Fig. 3I) were found in rats treated with DM compared to controls. Representative EEGs and their power spectra are shown in Fig. 3K. These results indicate that inhibiting SDH with DM partly reversed succinate accumulations and the increased oxidative stress levels attenuated the severity of seizure in KA-induced SE.

3.4. DM attenuated the elevated levels of mitophagy and neuronal degeneration induced by KA

We also explored the level of mitophagy and neuronal degeneration in the KA + DM/saline groups (n = 60). Hippocampal ($P < 0.001$, Fig. 4A–E) and cortical ($P < 0.001$, Fig. 4E) LC3B immunoreactivity levels were significantly reduced after treated with DM, as confirmed via immunohistochemistry. These observations of changes were also supported by Western blot results (Hippocampus: 24 h, $P = 0.015$; 3 days, $P = 0.005$ *vs.* Cortex: 24 h, $P = 0.045$; 3 days, $P = 0.007$; Fig. 4F and G). Additionally, FJB staining demonstrated decreased neuronal degeneration with DM compared with controls that were treated with saline ($P < 0.001$ Fig. 4H–J). These results revealed that DM interference significantly reduced the mitophagy and neuronal degeneration in KA-induced SE.

3.5. AOA reduced the succinate, DCF, and mito-SOX levels as well as seizures induced by KA

AOA is the most widely used and specific inhibitor of MAS [39].

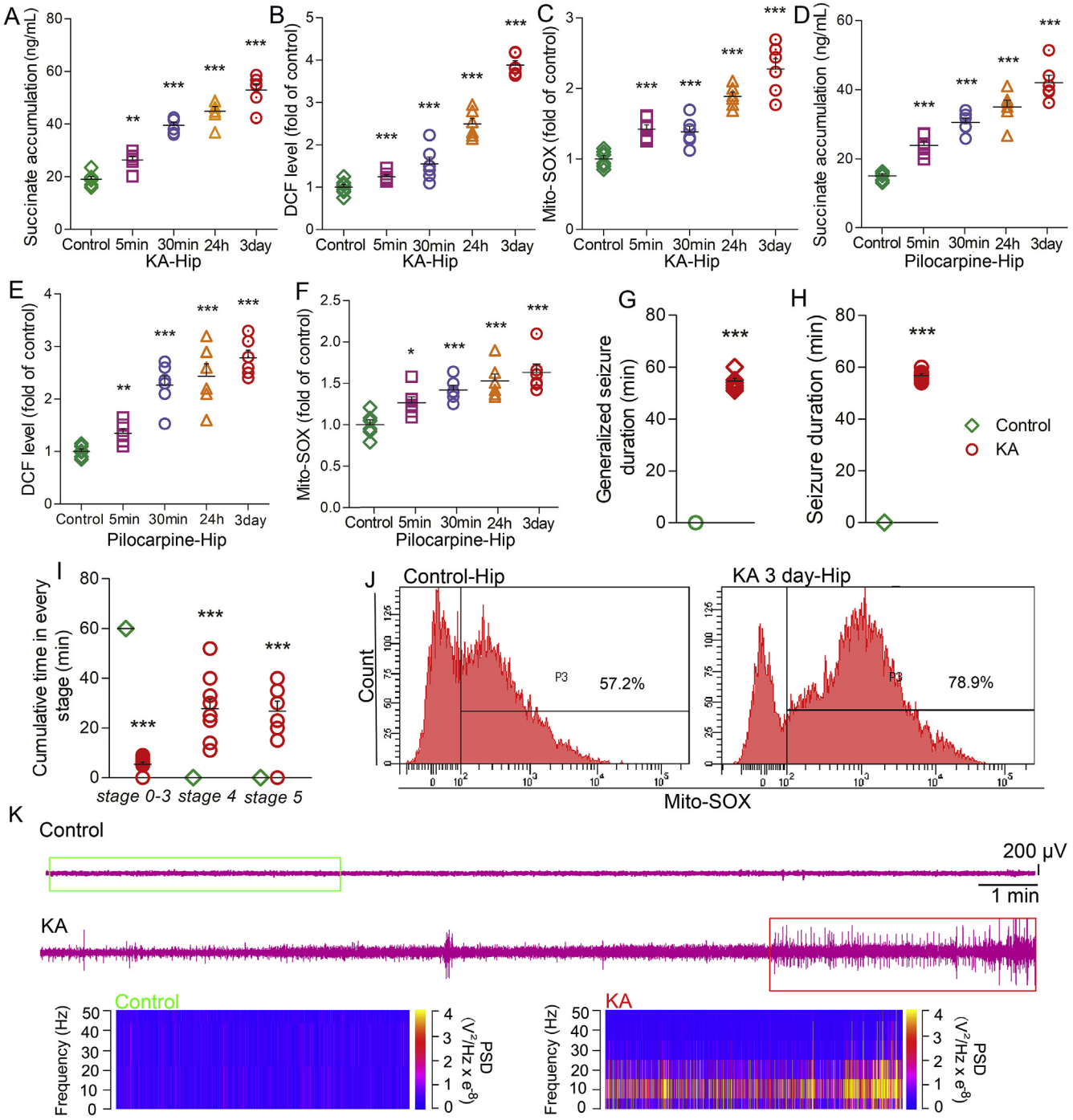

Fig. 1. Hippocampal succinate accumulation and increased DCF and mito-SOX levels in KA- or pilocarpine-induced SE

Hippocampal succinate (A, n = 6 per timepoint), DCF (B, n = 6 per timepoint),and mito-SOX (C, n = 6 per timepoint) levels were increased after 5 min of evoked seizures by kainic acid (KA). A similar increase was found after pilocarpine administration. (D) Succinate accumulation (n = 6 per timepoint); (E) DCF level, fold change relative to controls (n = 6 per timepoint); (F) mito-SOX was measured by fluorescence-activated cell using Mito-SOX dye, fold change relative to controls (n = 6 per timepoint). Evaluation of seizure severity (n = 10 in KA group and n = 10 in control group) via GSD (G), seizure duration (H), and cumulative time spent in each stage (I). Flow cytometry-based quantification of hippocampal mito-SOX signal was measured by fluorescence-activated cell using Mito-SOX dye (J, n = 6/group). (K) Representative EEGs, frequency spectra, and power spectrum densities (PSDs) of both groups. Means ± SEM are shown. The nonparametric Mann-Whitney *U* test was used to analyze the cumulative time spent in each seizure stage as well as changes in succinate, DCF, and mito-SOX levels. Comparisons of the seizure duration and GSD were made via one-way ANOVA. *P < 0.05, **P < 0.01 and ***P < 0.001 versus controls. Abbreviations: KA, kainic acid; Hip, hippocampus.

This drug inhibits the shuttling of key enzymes via aspartate amino-transferase. In AOA-treated animals (n = 56), we found rescues of hippocampal and cortical succinate, DCF, and mito-SOX accumulation induced by KA. This rescue of AOA treatment occurred as early as 5 min after KA administration (hippocampal succinate: P = 0.007; cortical succinate: P = 0.002; hippocampal DCF: P = 0.002; cortical DCF: P = 0.006; hippocampal mito-SOX: P = 0.022; cortical mito-SOX: P = 0.002; Fig. 5A–F). Similar changes in the levels of hippocampal and

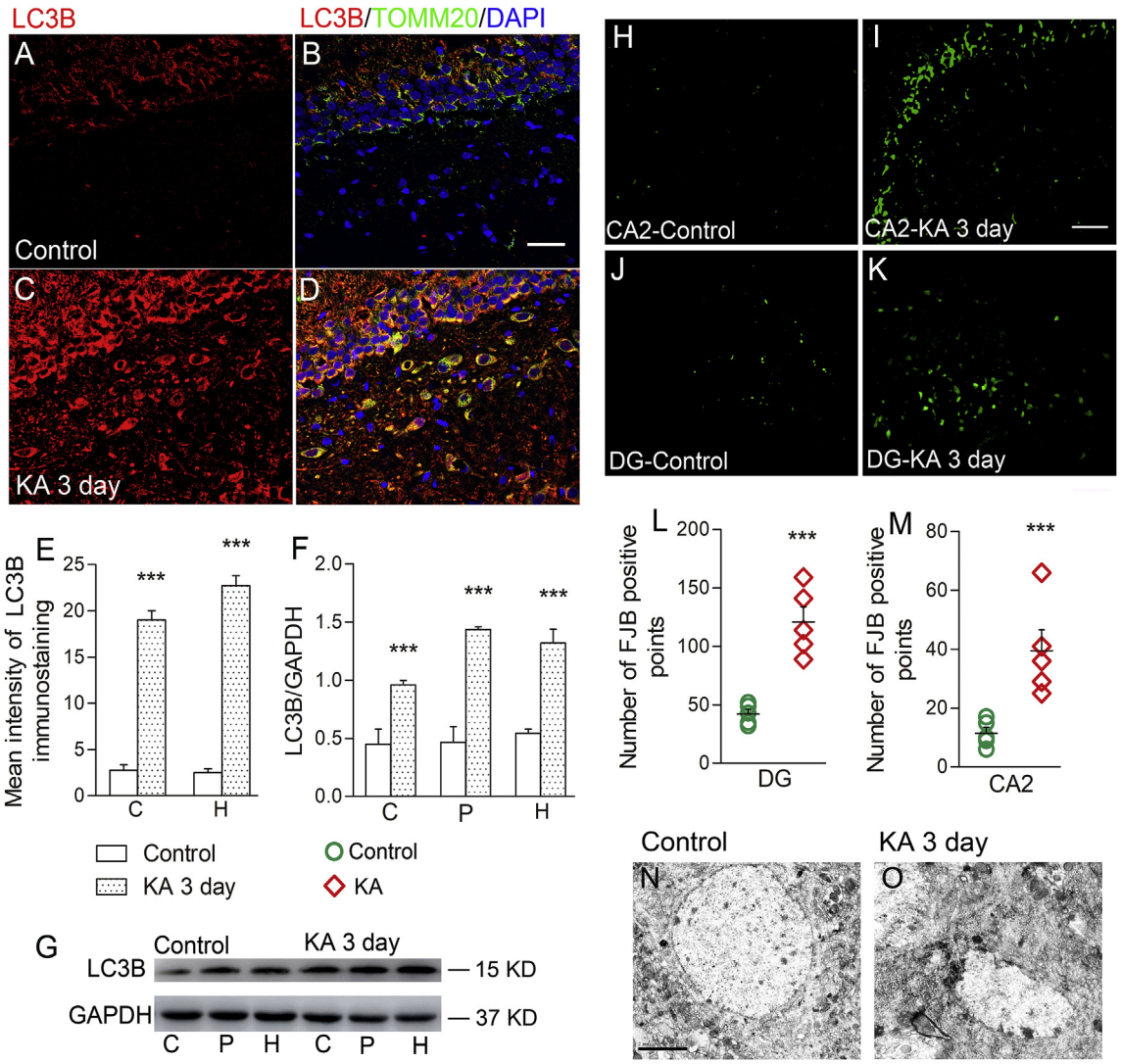

Fig. 2. Increased mitophagy and neuronal degeneration in rats with KA-induced SE
LC3B immunoreactivity was increased in the right CA1 after KA treatment relative to controls (A-E, n = 5/group). LC3B (red), TOMM20 (green) and DAPI (blue). LC3B expression in the hippocampus and cortex was detected by Western blot (F, G, n = 5/group). FJB staining was used to evaluate neuronal degeneration (H, I: CA2; J, K: DG, n = 5/group). The number of positive points of FJB staining (L, M). Neurons in DG were observed by transmission electron microscopy (N, O). Means ± SEM are shown. The nonparametric Mann-Whitney *U* test was used to analyze the protein expression. ***P < 0.001 versus controls. Abbreviations: C: cortex; H: hippocampus; P: piriform cortex; KA, kainic acid. (For interpretation of the references to color in this figure legend, the reader is referred to the Web version of this article.)

cortical mito-SOX signal after AOA treatment in KA-induced SE were found using flow cytometry (Fig. 5J).

Further evaluations of animal behavior and EEG patterns revealed that AOA-treated animals spent less time in stage 5 ($P < 0.001$; 40.3 ± 0.5 min *vs.* 12.1 ± 0.8 min; Fig. 5G) and more time in the less severe stages 0–3 ($P < 0.001$; 4.3 ± 0.4 min *vs.* 25.5 ± 1.1 min; Fig. 5G) and stage 4 ($P < 0.001$; 15.4 ± 0.4 min *vs.* 22.4 ± 0.9 min; Fig. 5G). Meanwhile, AOA led to shorter seizure duration ($P < 0.001$; 57.6 ± 0.3 min *vs.* 37.9 ± 1.0 min; Fig. 5I) and GSDs ($P < 0.001$; 55.7 ± 0.4 min *vs.* 34.5 ± 1.1 min; Fig. 5H). Representative EEGs and their power spectra after AOA treatment are shown in Fig. 5K.

3.6. AOA reduced the increased mitophagy and neuronal degeneration induced by KA

In another set of experiments, AOA (n = 60) was injected into the lateral ventricles. Western blots and immunohistochemical results revealed the changes of mitophagy in the hippocampus and cortex at 24h and 3 days after KA administration. We found that AOA interference significantly reduced mitophagy ($P < 0.001$, Fig. 6A–G). Furthermore, FJB staining demonstrated decreased KA-linked neurodegeneration with AOA ($P < 0.001$; Fig. 6H–J). These results demonstrate that AOA treatment significantly reduced mitophagy and neuronal degeneration in the KA rat SE model.

3.7. AICAR reduced the succinate, DCF/mito-SOX levels, and attenuated seizure severity

AICAR inhibits adenylosuccinate lyase in the PNC. AICAR treatment blocks the PNC pathway [30,40]. In AICAR-treated animals (n = 56), we found that KA-induced hippocampal (succinate: $P = 0.008$; DCF: $P = 0.027$; mito-SOX: $P = 0.018$) and cortical (succinate: $P = 0.002$; DCF: $P = 0.044$; mito-SOX: $P = 0.023$) DCF, mito-SOX and succinate accumulation were blocked with AICAR treatment at as early as the 5 min timepoint (Fig. 7A–F). Further experiments demonstrated that AICAR-treated animals spent less time in stage 5 ($P < 0.001$; 41.9 ± 0.8 min *vs.* 20.2 ± 0.7 min; Fig. 7G) and more time in stages 0–3 ($P < 0.001$; 4.6 ± 0.3 min *vs.* 19.8 ± 0.7 min; Fig. 7G). These

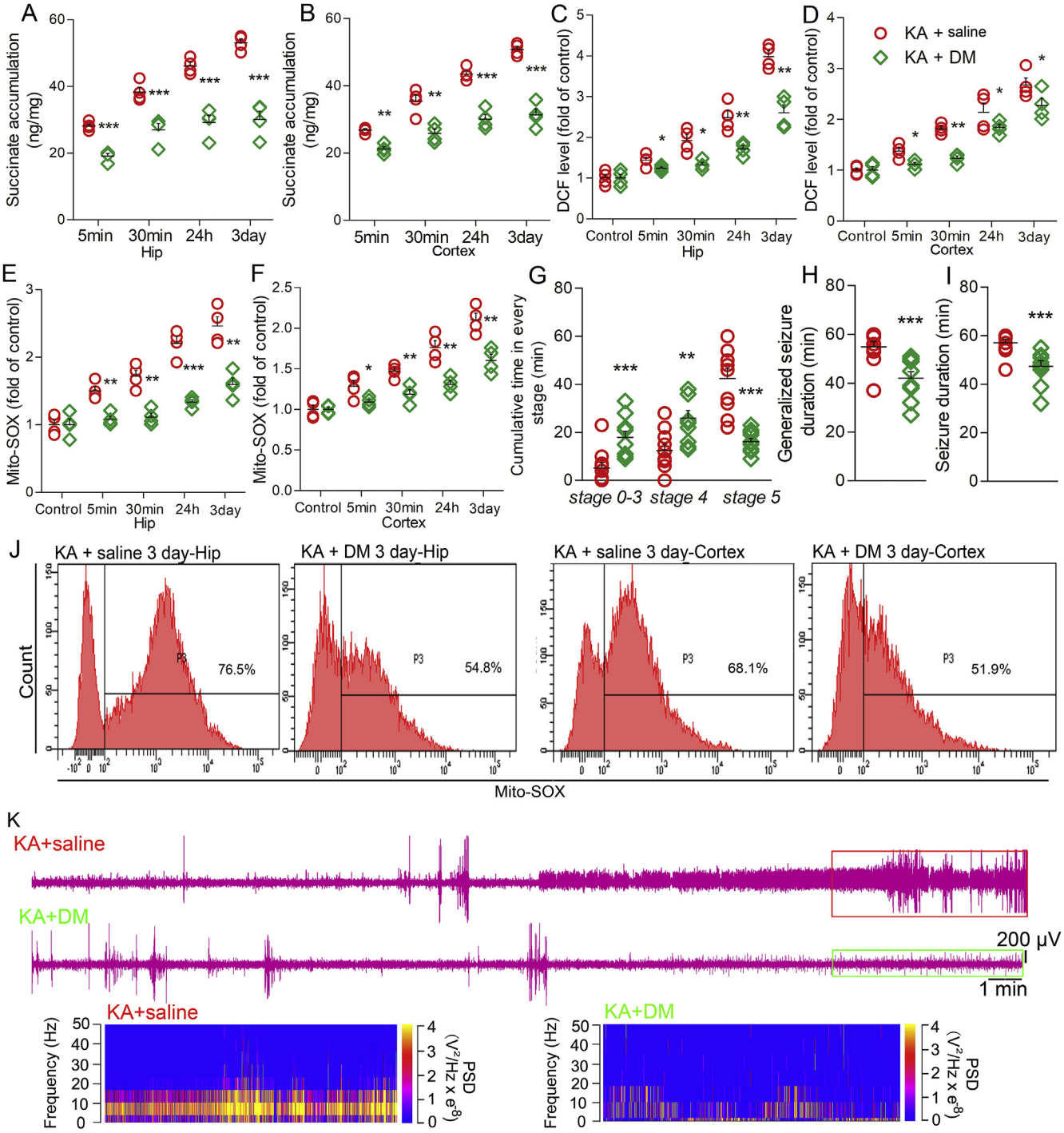

Fig. 3. DM, an SDH competitive inhibitor, reversed the elevated succinate and oxidative stress and reduced seizure severity in KA-treated mice
(A, B): Level of succinate accumulation (n = 4 per timepoint); (C, D): DCF level, fold change relative to controls (n = 4 per timepoint); (E, F): mito-SOX signal was measured by fluorescence-activated cell using Mito-SOX dye, fold change relative to controls (n = 4 per timepoint). Evaluation of seizure severity (n = 10 per group) by cumulative time spent in each stage (G), GSD (H), and seizure duration (I). Flow cytometry-based quantification of hippocampal and cortex mito-SOX signal was measured by fluorescence-activated cell using Mito-SOX dye (J, n = 4/group). (K) Representative EEG, frequency spectrum, and power spectrum density (PSD). Means ± SEM are shown. The nonparametric Mann-Whitney *U* test was used to analyze the cumulative time spent in each seizure stage as well as changes in succinate, DCF, and mito-SOX levels. Comparisons of seizure duration and GSD were made via one-way ANOVA. *P < 0.05, **P < 0.01 and ***P < 0.001 versus controls. Abbreviations: KA, kainic acid; Hip, hippocampus.

animals also had shorter GSDs (P < 0.001; 55.4 ± 0.3 min *vs.* 40.3 ± 0.7 min; Fig. 7H) and seizure duration (P < 0.001; 57.1 ± 0.2 min *vs.* 43.2 ± 0.7 min; Fig. 7I) than were observed in the control group. Similar changes in the levels of mito-SOX after AICAR treatment in KA-induced SE were found using flow cytometry (Fig. 7J). Representative EEGs and their power spectra after AICAR treatment are shown in Fig. 7K.

3.8. AICAR decreased the increased mitophagy and neuronal degeneration induced by KA

AICAR was injected into the lateral ventricles (n = 60). Western

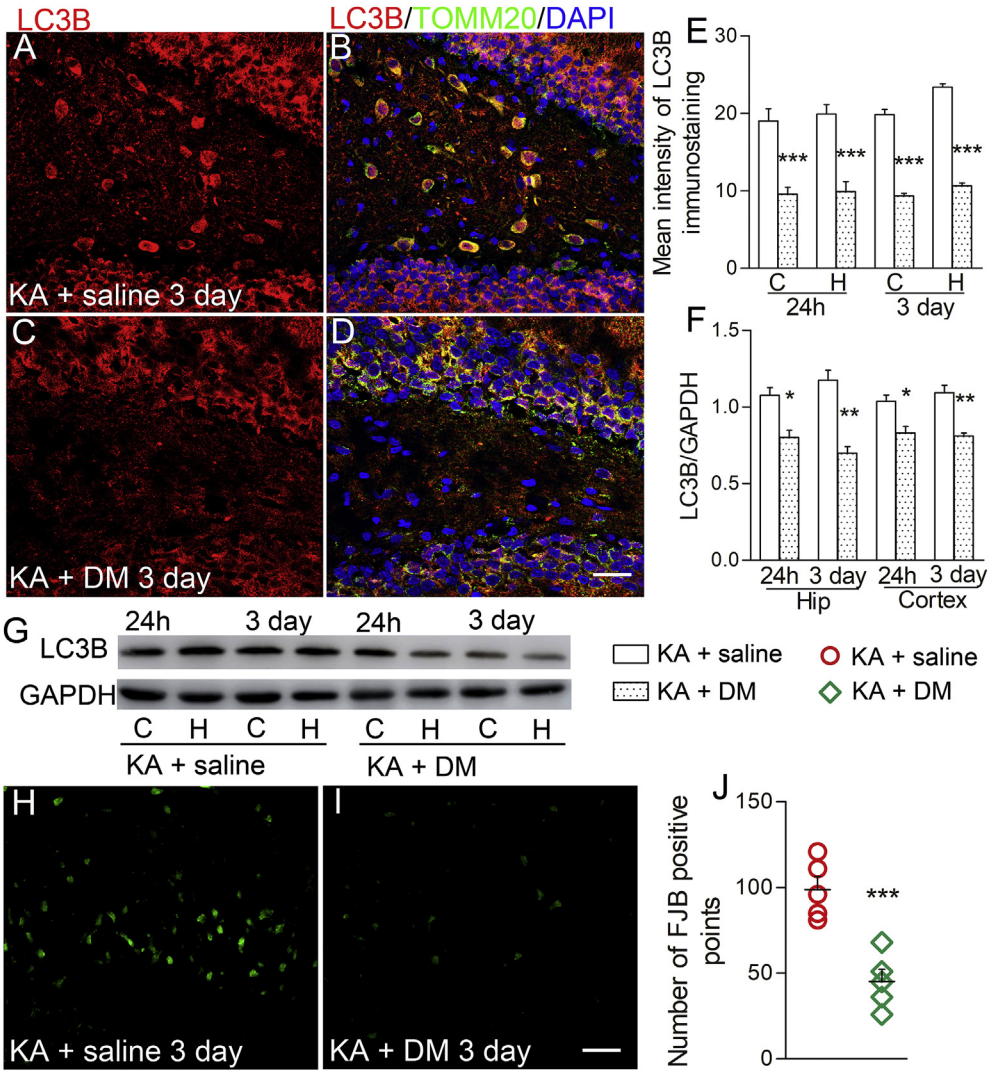

Fig. 4. DM attenuated the elevated mitophagy and neuronal degeneration induced by KA administration

(A-E) CA1 LC3B immunoreactivity was reduced after DM treatment (n = 5/group). LC3B (red), TOMM20 (green), and DAPI (blue). LC3B expression in the hippocampus and cortex by Western blot (F, G; n = 5/group). FJB staining was used to evaluate neuronal degeneration (H and I, n = 5/group). The number of positive points of FJB staining (J). Means ± SEM are shown. The nonparametric Mann-Whitney *U* test was used to analyze the expression of proteins. *P < 0.05, **P < 0.01 and ***P < 0.001 versus controls. Abbreviations: C: cortex; H: hippocampus; KA, kainic acid. (For interpretation of the references to color in this figure legend, the reader is referred to the Web version of this article.)

blots and immunohistochemical results revealed the changes of mitophagy in the hippocampus and cortex at the 24 h and 3-day timepoints. AICAR blockade significantly reduced mitophagy (P < 0.001, Fig. 8A–G). FJB results further revealed that neuronal degeneration was decreased with AICAR compared with that in the control group (P < 0.001; Fig. 8H–J). Collectively, these findings demonstrate that AICAR treatment significantly reduces mitophagy and neuronal degeneration in KA-induced SE.

3.9. SAD recapitulated KA-linked increases in succinate, DCF, and mito-SOX levels

SAD, which is used to induce succinate accumulation [41,42], was administered into the lateral ventricles to directly evaluate the relationship between succinate accumulation and oxidative stress levels and seizures. In SAD-treated animals (n = 32), hippocampal and cortical succinate accumulation were significantly increased at the detected timepoints (5 min and 30 min). Furthermore, DCF level increased with succinate accumulation (succinate: P < 0.001, Fig. 9A and B; DCF: P < 0.001, Fig. 9C and D), as well as increased mito-SOX level (P < 0.001, Fig. 9E and F). Similar changes in the levels of mito-SOX signal after SAD treatment were found using flow cytometry (Fig. 9I). We also found that SAD-treated animals spent more time in stage 2 (11.7 ± 0.8 min *vs.* 1.8 ± 0.2 min; P < 0.001; Figs. 9G) and 3 (7.4 ± 0.5 min *vs.* 0 min; P < 0.001; Fig. 9G) and less time in stage 0 (5.4 ± 0.4 min *vs.* 26.9 ± 0.3 min; P < 0.001; Fig. 9G) than DMSO-treated ones. Moreover, the seizure duration in the SAD group was significantly longer than that in the DMSO group (P < 0.001; Fig. 9H).

4. Discussion

The present study provides evidence that succinate accumulation likely plays a vital role in KA-induced SE. First, succinate accumulation accompanied by increased mito-SOX and oxidative stress levels were found in different SE rat models, as well as increased mitophagy and neurodegeneration. Next, we found that inhibiting SDH with DM significantly relieved succinate accumulation, accompanied by reduced oxidative stress, and mito-SOX levels, as well as attenuated neurodegeneration and the severity of seizures induced by KA. Moreover, a similar rescue effect was found in rats treated with AOA and AICAR, which block the MAS and PNC pathways, respectively. Supplementation with SAD, which increased succinate levels, led to succinate accumulation, as well as increased oxidative stress and mito-SOX levels and seizure phenotypes similar to those induced by KA in normal rats.

Mitochondria serve essential cellular roles, including regulation of intermediary metabolism and bioenergetics [43,44]. Critically, mitochondria share a close link with bioenergetics in epileptogenesis, which is supported by significant clinical data such as a patient with mitochondrial mutation always has associated epilepsy [45].

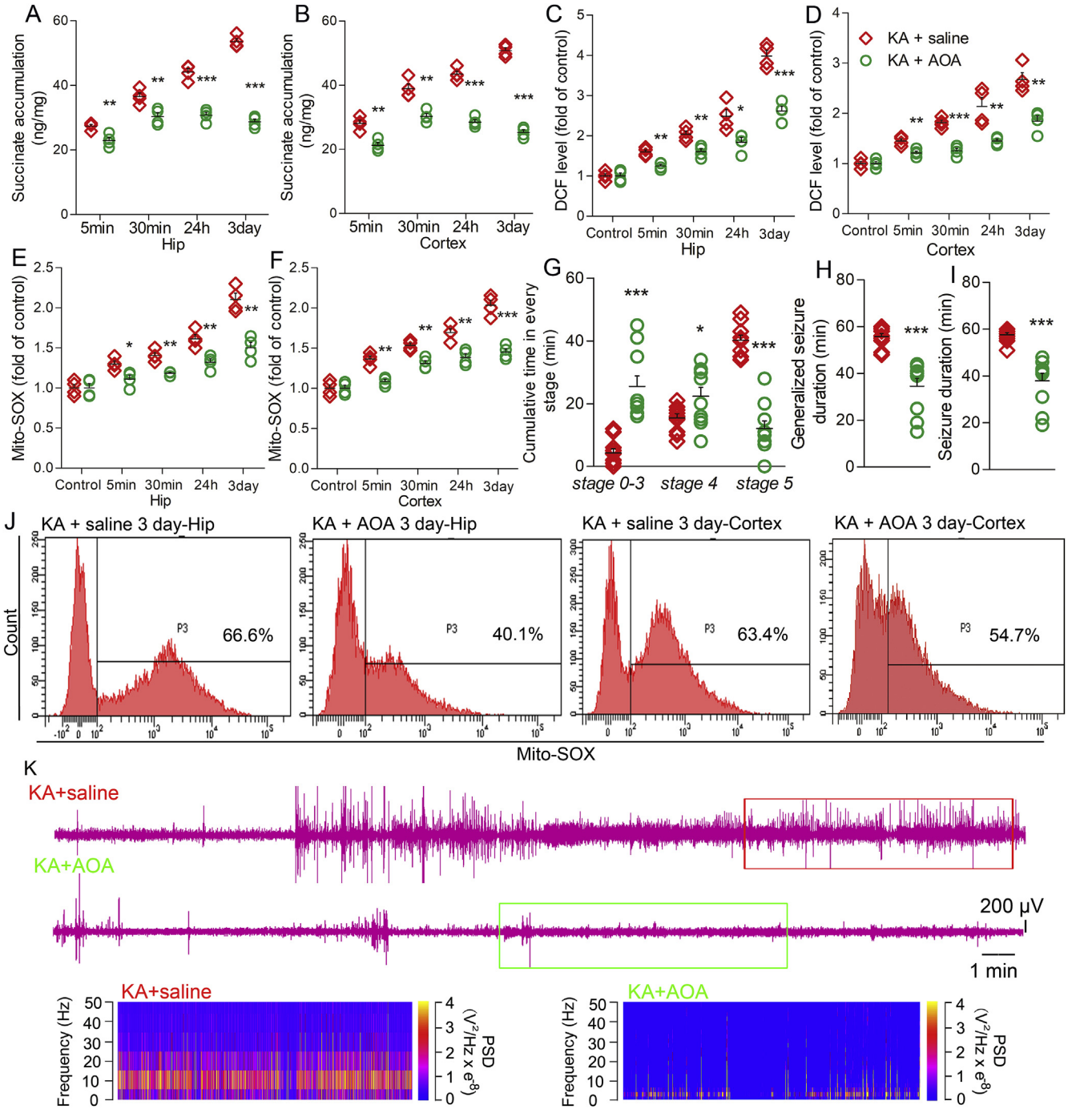

Fig. 5. AOA decreased succinate, DCF, and mito-SOX levels, and attenuated seizure severity in KA-induced SE
KA-induced increased succinate (A, B), DCF level (C, D) and mito-SOX (measured by Mito-SOX dye) (E, F) in the hippocampus and cortex was reversed with AOA (n = 4/group). Seizure severity of animals was attenuated after AOA treatment (G, cumulative time in every stage; H, GSD; and I, seizure duration; n = 10/group). Flow cytometry-based quantification of mito-SOX signal (J, n = 4/group). (K) Representative EEG, frequency spectrum, and power spectrum density (PSD). The nonparametric Mann-Whitney *U* test was used to analyze the cumulative time spent in each seizure stage as well as changes in succinate, DCF, and mito-SOX levels. Comparisons of the seizure duration and GSD were made via one-way ANOVA. Means ± SEM are shown. *P < 0.05, **P < 0.01 and ***P < 0.001 versus controls. Abbreviations: KA, kainic acid; Hip, hippocampus.

Mitochondrial dysfunction is thus a feature of epilepsy [46], with mitochondrial metabolic impairments and oxidative stress playing vital roles in the etiology and pathophysiology of epilepsy [47,48]. Recently, seizures were shown to result in mitochondrial oxidative stress due to excessive ROS production [5,6]. Oxidative damage to vulnerable mitochondrial and hippocampal molecules and even neuronal death have been found in multiple animal models of acquired epilepsy, such as glutamate agonist (e.g., KA), acetylcholine agonist (e.g., pilocarpine), electric kindling, and PTZ models [49–51]. Additional reports on KA treatment, lithium-pilocarpine, and PTZ-kindling models of epilepsy have all demonstrated that seizures result in increased ROS production [52,53]. The production of ROS, which is associated with mitochondrial defects, also impacts epileptogenesis [9,54].

Traditionally, mitochondria are thought to serve as the primary sites of ROS production during epileptic seizures. ROS are primarily generated by the mitochondrial ETC [5], although there are other sources of

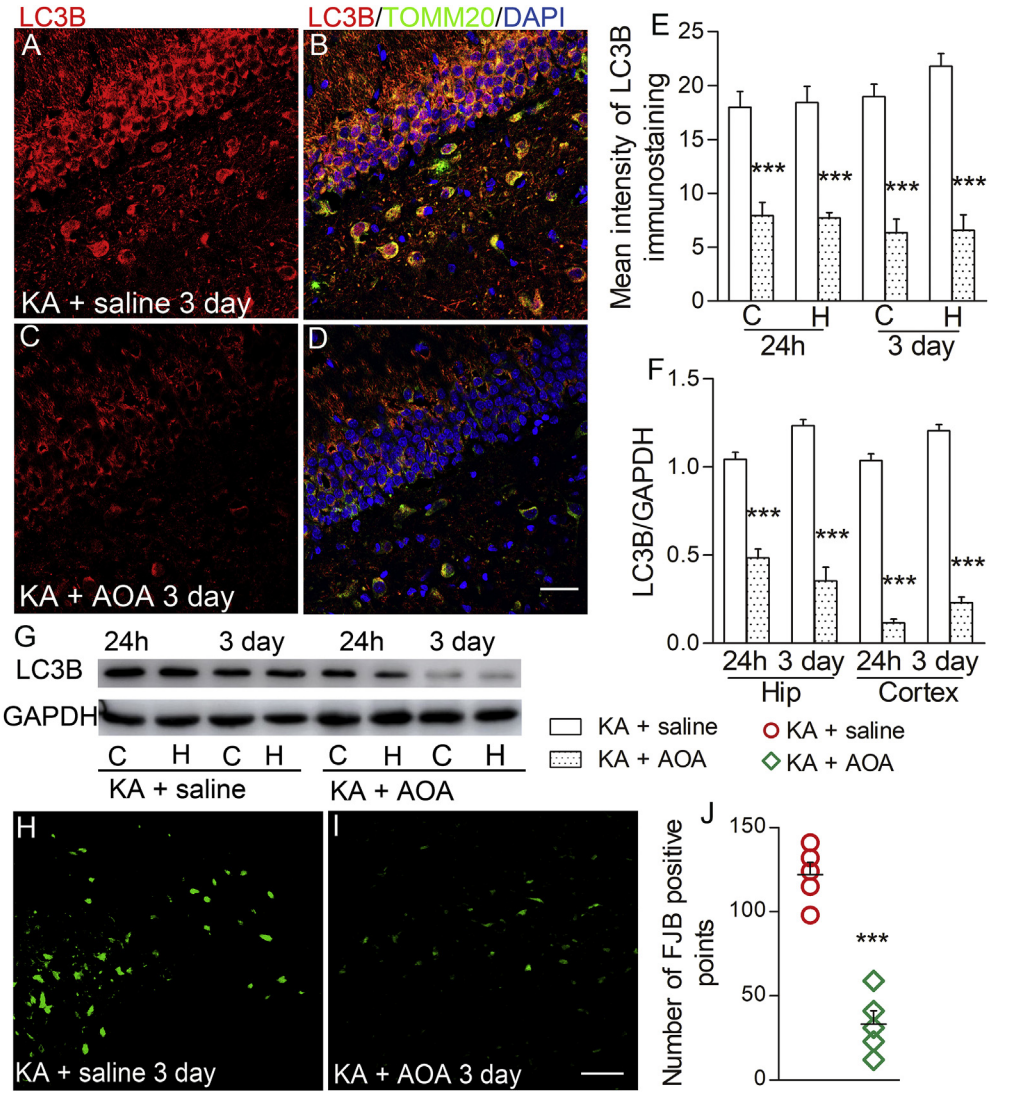

Fig. 6. AOA relieved mitophagy and neuronal degeneration induced by KA administration

(A-E) CA1 LC3B immunoreactivity was reduced with AOA treatment (n = 5/group). LC3B (red), TOMM20 (green), and DAPI (blue). LC3B expression in the hippocampus and cortex by Western blot (F, G; n = 5/group). FJB staining was used to evaluate neuronal degeneration (H and I, n = 5/group). The number of positive points of FJB staining (J). Means ± SEM are shown. The nonparametric Mann-Whitney *U* test was used to analyze the expression of proteins. ***P < 0.001 versus controls. Abbreviations: C: cortex; H: hippocampus; KA, kainic acid. (For interpretation of the references to color in this figure legend, the reader is referred to the Web version of this article.)

ROS such as xanthine oxidase, cyclooxygenase, and lipoxygenase [3,55–58].

Mitochondria, the main site of ROS production in the cell, are particularly vulnerable to oxidative damage, which may play a key role in controlling neuronal excitability [11]. Previous studies in animal models and human samples have shown that mitochondrial dysfunction is associated with epilepsy and SE [10,59]. The role of mitochondrial dysfunction in chronic epilepsy is complex, and it is difficult to determine whether mitochondrial oxidative stress is a cause or a consequence of seizures. However, recent studies have supported the contribution of mitochondrial oxidative stress in not only epileptic seizures but also epileptogenesis. Mitochondrial complex I deficiency may be the link between mitochondrial oxidative stress and epilepsy [11]. This relationship between mitochondrial dysfunction and epilepsy is further supported by the absence of mitochondrial complex I in the epileptic foci of some TLE patients [60].

Previous reports have provided some evidence that succinate accumulation is closely associated with mitochondrial ROS. One previous study referred to mitochondria as the major source of ROS. Approximately 50% of ROS production from brain mitochondria was associated with succinate-supported reverse electron transport (RET) [61]. Succinate generates ROS by driving RET at complex I [18]. Meanwhile, SDH (complex II), a key enzyme which is responsible for oxidizing succinate to fumarate, maintains ROS homeostasis in mitochondria through the balance of production and elimination of superoxide [23]. In specific pathological conditions [18,20], succinate is accumulated due to the reverse catalysis of SDH. Accumulated succinate is rapidly re-oxidized by SDH, subsequently driving excessive ROS production via mitochondrial complex I RET [25]. Meanwhile, previous research suggests that inhibition of complex II (SDH) may against ROS associated with RET [62]. Furthermore, SDH/complex II is the main source of electrons for ROS production, regardless of whether ROS arises from complexes I, II, or III [63]. Our study also confirmed that SDH competitive inhibitor (DM) reversed the elevated succinate and mito-SOX levels in KA-induced SE. Due to the vital contribution of SDH in the mitochondrial superoxide, we have reason to speculate that SDH may be the potential target for reducing mitochondrial ROS and mitochondrial ROS related pathological progression, such as neuronal injury and seizure.

The mechanism of SE is complex and ROS-induced oxidative stress is one important contributor [64]. Additionally, down regulated synaptic GABA(A) receptors, up regulated NMDA receptors [65–67], Ca^{2+}-induced release of glutamate and/or D-serine [68–70], protein kinase C, AKT and extracellular signal-related kinases 1/2 (ERK1/2) [71] may also be involved. In our study, we found that succinate accumulations occurred concomitantly with increased DCF and mito-SOX signal in the SE rats. Moreover, this increase in DCF and mito-SOX was partially reversed when succinate accumulation was reduced. As an ROS marker, DCF-DA is used to assess oxidative stress [72–74], though there are some limitations to this technique. For example, DCF

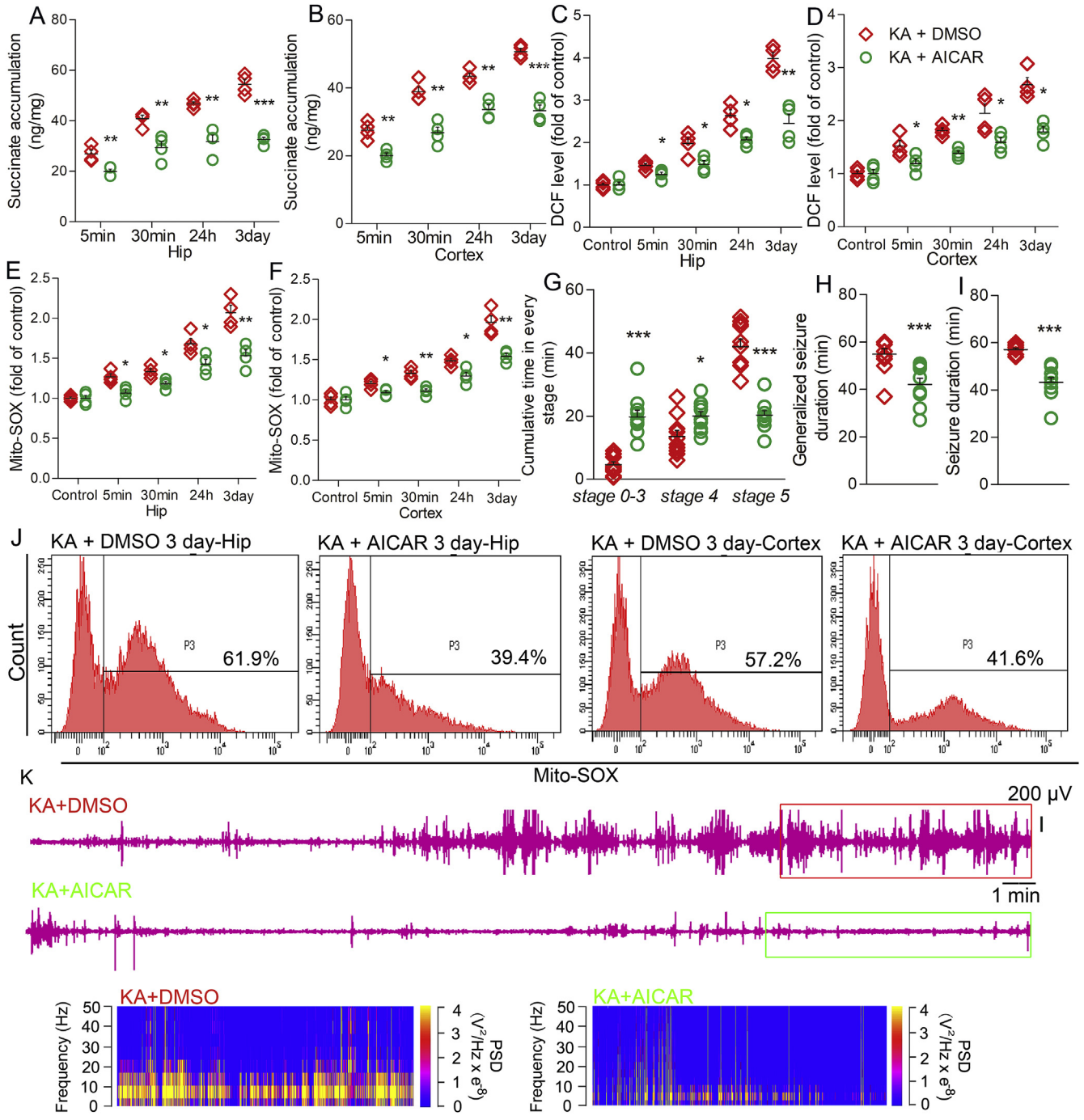

Fig. 7. AICAR decreased succinate, DCF and mito-SOX levels, and relieved KA-induced seizureIncreased levels of succinate (A, B), DCF level (C, D), and mito-SOX (E, F) induced by KA administration in the hippocampus and cortex were reversed by AICAR treatment (n = 4/group). Seizure severity was attenuated with AICAR treatment (G, cumulative time in every stage; H, GSD; and I, seizure duration; n = 10/group). Flow cytometry-based quantification of mito-SOX signal (J, n = 4/group). Means ± SEM are shown. The nonparametric Mann-Whitney *U* test was used to analyze the cumulative time spent in each seizure stage as well as changes in succinate, DCF, and mito-SOX levels. Comparisons of the seizure duration and GSD were made via one-way ANOVA. *P < 0.05, **P < 0.01 and ***P < 0.001 versus controls. Abbreviations: KA, kainic acid; Hip, hippocampus.

fluorescence cannot be used as a direct measure of H_2O_2, and is prone to multiple artifacts and artifactual amplification in ROS analysis [75]. Our results indicate that for succinate accumulations may contribute to the increased mitochondrial ROS and oxidative stress in KA-induced SE. Due to the possible influence by cellular superoxide, results from mito-SOX measurements only indicate the mitochondrial superoxide level. The potential pathological role of succinate in mitochondrial superoxide will be further validated by specific scavengers, such as, mito-TEMPO.

Mitophagy also plays a possible critical role in ROS-mediated brain dysfunction, such as epilepsy. Mitophagy describes a process of autophagy degradation mediated by mitochondria and lysosomes. This process is used to clear out dysfunctional mitochondria from cells and is thus important for maintaining a "healthy" pool of intracellular mitochondria [76,77]. It is reported that mitochondrial injury may activate mitophagy in refractory TLE, leading to the clearance of mitochondria themselves [78]. Previous studies have reported that central nervous system mitochondrial dysfunction may lead to epileptic

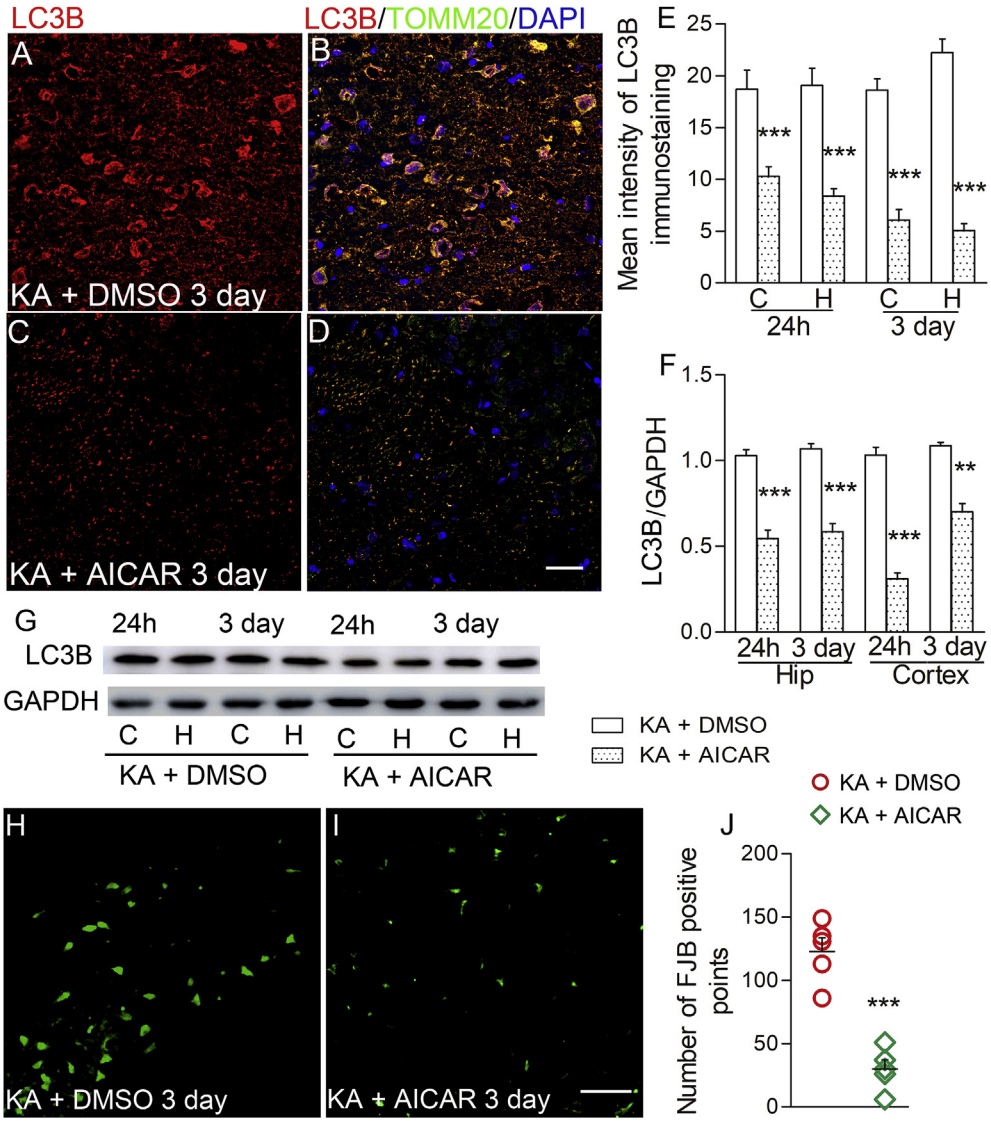

Fig. 8. AICAR partly reversed the increased mitophagy and neuronal degeneration caused by KA administration
(A-E) CA1 LC3B immunoreactivity was reduced with AICAR treatment (n = 5/group). LC3B (red), TOMM20 (green), and DAPI (blue). LC3B expression in the hippocampus and cortex by Western blot (F, G; n = 5/group). FJB staining was used to evaluate neuronal degeneration. (H, KA + DMSO at 3 days; I, KA + AICAR at 3 days; n = 5/group). The amount of positive points of FJB staining (J). Means ± SEM are shown. The nonparametric Mann-Whitney *U* test was used to analyze the expression of protein. **P < 0.01 and ***P < 0.001 versus controls. Abbreviations: C: cortex; H: hippocampus; KA, kainic acid. (For interpretation of the references to color in this figure legend, the reader is referred to the Web version of this article.)

seizures [79,80]. Moreover, mitochondrial dysfunction not only leads to altered energy consumption but also changes transient Ca^{2+} states and results in the release of harmful ROS causing neurons to degenerate and even die [8,81].

Mitophagy plays a key role in controlling mitochondrial quality by removing damaged or redundant mitochondria [8,79]. Our results further indicate that LC3B immunoreactivity, a marker of mitophagy, is increased synchronously with increased levels of succinate, oxidative stress, and mito-SOX in KA-induced SE. Moreover, inhibiting the accumulation of succinate may reverse these LC3B increases. Collectively, these results indicate that succinate accumulation-induced mitophagy, which may be due to increased oxidative stress and mitochondrial ROS, contributes to the KA-induced SE.

Recent reports have indicated the possible sources of succinate accumulation. The first is the inverse catalysis of SDH. Though succinate is dehydrogenated by SDH to generate fumarate in normal cells, the inverse catalysis of SDH has been reported during ischemia, resulting in neuronal damage during reperfusion as electrons flow in reverse through complex I, generating ROS [25]. Under this pathological condition, fumarate is upstream of succinate. When the NADH/NAD^+ ratio (complex I) is high, the MAS and PNC pathways are activated. These two pathways may also be responsible for succinate accumulation in ischemia/reperfusion injury models [18]. Inhibiting the inverse catalysis of SDH via the MAS or PNC may reduce succinate accumulation, thus avoiding subsequent ROS damage [18], which is closely associated with epileptogenesis and epileptic seizures [82]. The results of the present study demonstrate that increased levels of succinate may be responsible for elevated oxidative stress in rats with KA-induced SE. Furthermore, the accumulation of succinate is mainly due to the inverse catalysis of SDH from fumarate, which is supplemented by the MAS and PNC pathways.

The main reason for succinate accumulation is the reverse activity of SDH, though other metabolic pathways, such as glycolysis, glutaminolysis, and GABA shunting may also participate in succinate accumulation [18]. However, glycolysis and glutaminolysis induce the accumulation of succinate constrained by the overproduction of NADH. Thus, the contributions of glycolysis and glutaminolysis to succinate accumulations are small [18].

Succinate is closely related to GABA. GABA is synthesized by glutamic acid decarboxylase from glutamate, with pyridoxal phosphate (the active form of vitamin B6) serving as a cofactor [83]. Given this, GABA is a metabolite of glutamate mainly via the TCA cycle [84]. Subsequently, aminobutyric acid transaminase converts GABA into succinic-semialdehyde, which is further oxidized by succinic acid-hemialdehyde dehydrogenase to succinate.

Furthermore, succinate is a butene diacid isomer that is similar in structure to glutamate and GABA [85]. Succinate is an important feature of the Krebs cycle and the glutamate-GABA shunt [86], as

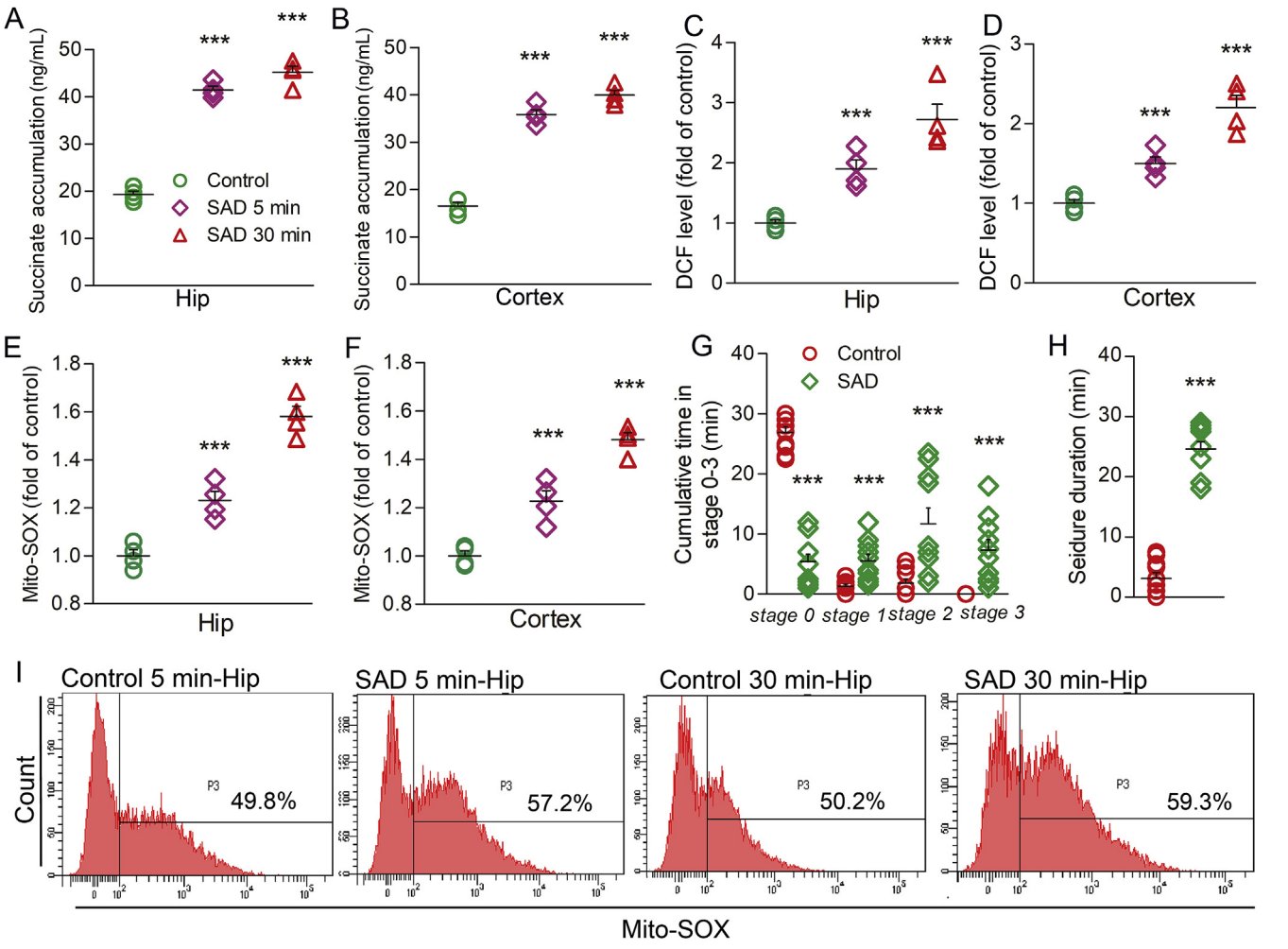

Fig. 9. SAD induced succinate, DCF, and mito-SOX accumulation and simulated the seizures similar to those induced by KA administration
Increased levels of succinate (A, B), DCF level (C, D), and mito-SOX (E, F) in the hippocampus and cortex were found after SAD administration (n = 4/group). Seizure behaviors (G, H) were induced by SAD (n = 10/group). Flow cytometry-based quantification of hippocampal mito-SOX signal (I, n = 4/group). Means ± SEM are shown. The nonparametric Mann-Whitney *U* test was used to analyze the cumulative time spent in each seizure stage as well as changes in succinate, DCF, and mito-SOX levels. Comparison of the seizure duration was made via one-way ANOVA. ***P < 0.001 versus controls. Abbreviations: KA, kainic acid; Hip, hippocampus.

mentioned above. Glutamate, GABA, and succinate can also mutually transform with the action of particular enzymes [84]. Clinically, the treatment of epilepsy is usually dependent on increased GABAergic inhibition in the brain [85]. Evidence suggests that succinate inhibits kindling by enhancing GABA(a) subtype receptors in PTZ-induced and amygdala kindling models of epilepsy [87]. However, some studies have also found that succinate behaves as a partial NMDA agonist and increases post-synaptic neuronal excitatory *in vitro*, thereby inducing convulsions [88]. SDH inhibitors may also cause neurotoxic effects and selective neuronal death [89–91].

Our results further confirm that succinate accumulation may underlie the neuronal injury and SE induced by KA. Based on the diverse results discussed here, we contend that, due to mutual transformations between succinate, GABA, and glutamate, the effect of succinate may differ across physiological and pathological processes [92]. For example, in the normal TCA, SDH catalyzes the oxidation of succinate into fumarate, with an SDH inhibitor resulting in succinate accumulation. However, in some pathological process, succinate accumulates from fumarate via SDH reverse catalysis [18]. Moreover, we speculate that the succinate accumulation may break the balance of GABA/glutamate and further contribute to the pathology of SE induced by KA administration in our study.

5. Conclusions

In summary, the present study provides evidence for the possible role of succinate accumulation in the mitochondrial ROS production, oxidative stress, mitophagy, neurodegeneration, as well as seizures in the KA-induced SE rat model. Accumulations of succinate were mainly due to the inverse catalysis of SDH from fumarate, which is sourced from the MAS and the PNC. Additionally, reversing these succinate accumulations significantly reduced oxidative stress, attenuated resulting neurodegeneration, and decreased the severity of seizures induced by KA. These results provide new insights into the mechanisms underlying SE and indicate that decreasing succinate accumulation may be a therapeutic target for the treatment of SE. Based on the complex effects of succinate, further studies are required to assess its precise contributions to seizures and epilepsy in human populations.

Author contributions

YR Z and MD Z: study conception and design, data acquisition. W Z, J Y, and QY W: KA-induced rat model preparation and pharmacological manipulations. JJ Z, YR C, XH P, and X G: data acquisition and analysis. HL S: study design, data acquisition, and drafting of the manuscript.

Declaration of competing interest

None.

Acknowledgments

We would like to thank Editage for English language editing.

Appendix A. Supplementary data

Supplementary data to this article can be found online at https://doi.org/10.1016/j.redox.2019.101365.

Funding

This study was funded by the National Natural Science Foundation of China (grant number: 81573412), Key Research and Development Plan of Shandong Province (grant number: 2018GSF121004), and Yantai City (grant numbers: 2019XDHZ098).

References

[1] H.L. Sun, L.Y. Ma, Y.R. Zhang, X.H. Pan, C.Y. Wang, J.J. Zhang, X.L. Zhang, H.W. Sun, Q.Y. Wang, W. Zhu, A purinergic P2 receptor family-mediated increase in thrombospondin-1 bolsters synaptic density and epileptic seizure activity in the amygdala-kindling rat model, Front. Cell. Neurosci. 12 (2018) 302, https://doi.org/10.3389/fncel.2018.00302.

[2] D. Malinska, B. Kulawiak, A.P. Kudin, R. Kovacs, C. Huchzermeyer, O. Kann, C. Huchzermeyer, O. Kann, A. Szewczyk, W.S. Kunz, Complex III-dependent superoxide production of brain mitochondria contributes to seizure-related ROS formation, Biochim. Biophys. Acta 1797 (2010) 1163–1170, https://doi.org/10.1016/j.bbabio.2010.03.001.

[3] S. Kovac, A.T. Dinkova-Kostova, A.Y. Abramov, The role of reactive oxygen species in epilepsy, React. Oxyg. Species 1 (2016) 38–52, https://doi.org/10.1016/j.neuroscience.2015.07.005.

[4] L.P. Liang, J.N. Pearson-Smith, J. Huang, B.J. Day, M. Patel, Neuroprotective effects of a catalytic antioxidant in a rat nerve agent model, Redox Biol. 20 (2019) 275–284, https://doi.org/10.1016/j.redox.2018.10.010.

[5] A. Das, M. McDowell, C.M. O'Dell, M.E. Busch, J.A. Smith, S.K. Ray, N.L. Banik, Post-treatment with voltage-gated Na(+) channel blocker attenuates kainic acid-induced apoptosis in rat primary hippocampal neurons, Neurochem. Res. 35 (2010) 2175–2183, https://doi.org/10.1007/s11064-010-0321-1.

[6] D.C. Henshall, T. Araki, C.K. Schindler, J.Q. Lan, K.L. Tiekoter, W. Taki, R.P. Simon, Activation of Bcl-2-associated death protein and counter-response of Akt within cell populations during seizure-induced neuronal death, J. Neurosci. 22 (2002) 8458–8465, https://doi.org/10.1523/JNEUROSCI.22-19-08458.2002.

[7] M.A. Souza, B.C. Mota, R.R. Gerbatin, F.S. Rodriques, M. Castro, M.R. Fiqhera, L.F. Royes, Antioxidant activity elicited by low dose of caffeine attenuates pentylenetetrazol-induced seizures and oxidative damage in rats, Neurochem. Int. 62 (2013) 821–830, https://doi.org/10.1016/j.neuint.2013.02.021.

[8] N. Hattori, S. Saiki, Y. Imai, Regulation by mitophagy, Int. J. Biochem. Cell Biol. 53 (2014) 147–150, https://doi.org/10.1016/j.biocel.2014.05.012.

[9] D. Boison, C. Steinhäuser, Epilepsy and astrocyte energy metabolism, Glia 66 (2018) 1235–1243, https://doi.org/10.1002/glia.23247.

[10] S.D. Chen, A.Y. Chang, Y.C. Chuang, The potential role of mitochondrial dysfunction in seizure-associated cell death in the hippocampus and epileptogenesis, J. Bioenerg. Biomembr. 42 (2010) 461–465, https://doi.org/10.1007/s10863-010-9321-8.

[11] S. Waldbaum, M. Patel, Mitochondria, oxidative stress, and temporal lobe epilepsy, Epilepsy Res. 88 (2010) 23–45, https://doi.org/10.1016/j.eplepsyres.2009.09.020.

[12] S. Rowley, L.P. Liang, R. Fulton, T. Shimizu, B. Day, M. Patel, Mitochondrial respiration deficits driven by reactive oxygen species in experimental temporal lobe epilepsy, Neurobiol. Dis. 75 (2015) 151–158, https://doi.org/10.1016/j.nbd.2014.12.025.

[13] F. Scialò, A. Sriram, D. Fernández-Ayala, N. Gubina, M. Lõhmus, G. Nelson, A. Logan, H.M. Cooper, P. Navas, J.A. Enríquez, Mitochondrial ROS produced via reverse electron transport extend animal lifespan, Cell Metabol. 23 (2016) 725–734, https://doi.org/10.1016/j.cmet.2016.03.009.

[14] A. Sanz, P. Caro, J. Ibañez, J. Gómez, R. Gredilla, G. Barja, Dietary restriction at old age lowers mitochondrial oxygen radical production and leak at complex I and oxidative DNA damage in rat brain, J. Bioenerg. Biomembr. 37 (2005) 83–90, https://doi.org/10.1007/s10863-005-4131-0.

[15] N.S. Chandel, D.S. McClintock, C.E. Feliciano, T.M. Wood, J.A. Melendez, A.M. Rodriguez, P.T. Schumacker, Reactive oxygen species generated at mitochondrial complex III stabilize hypoxia-inducible factor-1alpha during hypoxia: a mechanism of O2 sensing, J. Biol. Chem. 275 (2000) 25130–25138, https://doi.org/10.1074/jbc.M001914200.

[16] E.L. Mills, B. Kelly, A. Logan, A.S.H. Costa, M. Varma, C.E. Bryant, P. Tourlomousis, J.H.M. Däbritz, E. Gottlieb, I. Latorre, Succinate dehydrogenase supports metabolic repurposing of mitochondria to drive inflammatory macrophages, Cell 167 (2016) 457–470, https://doi.org/10.1016/j.cell.2016.08.064.

[17] S. Vielhaber, H.G. Niessen, G. Debska-Vielhaber, A.P. Kudin, J. Wellmer, J. Kaufmann, M.A. Schönfeld, R. Fendrich, W. Willker, Subfield-specific loss of hippocampal N-acetyl aspartate in temporal lobe epilepsy, Epilepsia 49 (2008) 40–50, https://doi.org/10.1111/j.1528-1167.2007.01280.x.

[18] E.T. Chouchani, V.R. Pell, E. Gaude, D. Aksentijević, S.Y. Sundier, E.L. Robb, A. Logan, S.M. Nadtochiy, E.N.J. Ord, A.C. Smith, Ischaemic accumulation of succinate controls reperfusion injury through mitochondrial ROS, Nature 515 (2014) 431–435, https://doi.org/10.1038/nature13909.

[19] L.B. Valdez, T. Zaobornyj, M.J. Bandez, J.M. López-Cepero, A. Boveris, A. Navarro, Complex I syndrome in striatum and frontal cortex in a rat model of Parkinson disease, Free Radic. Biol. Med. 135 (2019) 274–282, https://doi.org/10.1016/j.freeradbiomed.2019.03.001.

[20] T.N. Andrienko, P. Pasdois, G.C. Pereira, M.J. Ovens, A.P. Halestrap, The role of succinate and ROS in reperfusion injury - a critical appraisal, J. Mol. Cell. Cardiol. 110 (2017) 1–14, https://doi.org/10.1016/j.yjmcc.2017.06.016.

[21] J. Li, Y.L. Yang, L.Z. Li, L. Zhang, Q. Liu, K. Liu, P. Li, B. Liu, L.W. Qi, Succinate accumulation impairs cardiac pyruvate dehydrogenase activity through GRP91-dependent and independent signaling pathways: therapeutic effects of ginsenoside Rb1, Biochim. Biophys. Acta (BBA) - Mol. Basis Dis. 1863 (2017) 2835–2847, https://doi.org/10.1016/j.bbadis.2017.07.017.

[22] J. Xu, H. Pan, X. Xie, J. Zhang, Y. Wang, G. Yang, Inhibiting succinate dehydrogenase by dimethyl malonate alleviates brain damage in a rat model of cardiac arrest, Neuroscience 393 (2018), https://doi.org/10.1016/j.neuroscience.2018.09.041 24-3.

[23] L. Tretter, A. Patocs, C. Chinopoulos, Succinate, an intermediate in metabolism, signal transduction, ROS, hypoxia, and tumorigenesis, Biochim. Biophys. Acta 1857 (2016) 1086–1101, https://doi.org/10.1016/j.bbabio.2016.03.012.

[24] C. Chinopoulos, Which way does the citric acid cycle turn during hypoxia? The critical role of α-ketoglutarate dehydrogenase complex, J. Neurosci. Res. 91 (2013) 1030–1043 https://doi:10.1002/jnr.23196.

[25] J.A. Boylston, J. Sun, Y. Chen, M. Gucek, M.N. Sack, E. Murphy, Characterization of the cardiac succinylome and its role in ischemia-reperfusion injury, J. Mol. Cell. Cardiol. 88 (2015) 73–81, https://doi.org/10.1016/j.yjmcc.2015.09.005.

[26] S. Huang, A.H. Millar, Succinate dehydrogenase: the complex roles of a simple enzyme, Curr. Opin. Plant Biol. 16 (2013) 344–349, https://doi.org/10.1016/j.pbi.2013.02.007.

[27] E. Easlon, F. Tsang, C. Skinner, C. Wang, S.J. Lin, The malate-aspartate NADH shuttle components are novel metabolic longevity regulators required for calorie restriction-mediated life span extension in yeast, Genes Dev. 22 (2008) 931–944 http://www.genesdev.org/cgi/doi/10.1101/gad.1648308.

[28] J.T. Barron, L. Gu, J.E. Parrillo, Malate-aspartate shuttle, cytoplasmic NADH redox potential, and energetics in vascular smooth muscle, J. Mol. Cell. Cardiol. 30 (1998) 1571–1579, https://doi.org/10.1006/jmcc.1998.0722.

[29] G. Van den Berghe, M.F. Vincent, J. Jaeken, Inborn errors of the purine nucleotide cycle: adenylosuccinase deficiency, J. Inherit. Metab. Dis. 20 (1997) 193–202.

[30] V. Sridharan, J. Guichard, C.Y. Li, R. Muise-Helmericks, C.C. Beeson, G.L. Wright, O (2)-sensing signal cascade: clamping of O(2) respiration, reduced ATP utilization, and inducible fumarate respiration, Am. J. Physiol. Cell Physiol. 295 (2008) C29–C37, https://doi.org/10.1152/ajpcell.00466.2007.

[31] H.L. Sun, W. Zhu, Y.R. Zhang, X.H. Pan, J.R. Zhang, X.M. Chen, Y.X. Liu, S.C. Li, Q.Y. Wang, D.P. Deng, Altered glutamate metabolism contributes to anti-epileptogenic effects in the progression from focal seizure to generalized seizure by low-frequency stimulation in the ventral hippocampus, Epilepsy Behav. 68 (2017) 1–7, https://doi.org/10.1016/j.yebeh.2016.09.009.

[32] R.J. Racine, Modification of seizure activity by electrical stimulation. II. Motor seizure, Electroencephalogr. Clin. Neurophysiol. 32 (1972) 281–294.

[33] S. Sagliocchi, A.G. Cicatiello, E. Di Cicco, R. Ambrosio, C. Miro, D. Di Girolamo, A. Nappi, G. Mancino, M.A. De Stefano, The thyroid hormone activating enzyme, type 2 deiodinase, induces myogenic differentiation by regulating mitochondrial metabolism and reducing oxidative stress, Redox Biol. 24 (2019), https://doi.org/10.1016/j.redox.2019.101228 101228.

[34] H.L. Sun, S.H. Zhang, K. Zhong, Z.H. Xu, B. Feng, J. Yu, Q. Fang, S. Wang, D.C. Wu, J.M. Zhang, Z. Chen, A transient upregulation of glutamine synthetase in the dentate gyrus is involved in epileptogenesis induced by amygdala kindling in the rat, PLoS One 8 (2013) e66885, , https://doi.org/10.1371/journal.pone.0066885.

[35] Y. Zhang, W. Zhu, H. Yu, J. Yu, M. Zhang, X. Pan, X. Gao, Q. Wang, H. Sun, P2Y4/TSP-1/TGF-β1/pSmad2/3 pathway contributes to acute generalized seizures induced by kainic acid, Brain Res. Bull. 149 (2019) 106–119, https://doi.org/10.1016/j.brainresbull.2019.04.004.

[36] L.C. Schmued, K.J. Hopkins, Fluoro-Jade B: a high affinity fluorescent marker for the localization of neuronal degeneration, Brain Res. 874 (2000) 123–130, https://doi.org/10.1016/S0006-8993(00)02513-0.

[37] L.C. Schmued, C.C. Stowers, A.C. Scallet, L. Xu, Fluoro-Jade C results in ultra high resolution and contrast labeling of degenerating neurons, Brain Res. 1035 (2005) 24–31, https://doi.org/10.1016/j.brainres.2004.11.054.

[38] D. Narendra, A. Tanaka, D.F. Suen, R.J. Youle, Parkin is recruited selectively to impaired mitochondria and promotes their autophagy, J. Cell Biol. 183 (2008) 795–803, https://doi.org/10.1083/jcb.200809125.

[39] N.R. Jespersen, T. Yokota, N.B. Støttrup, A. Bergdahl, K.B. Paelestik, J.A. Povlsen, F. Dela, H.E. Bøtker, Pre-ischaemic mitochondrial substrate constraint by inhibition of malate-aspartate shuttle preserves mitochondrial function after ischaemia-reperfusion, J. Physiol. 595 (2017) 3765–3780, https://doi.org/10.1113/JP273408.

[40] J.L. Swain, J.J. Hines, R.L. Sabina, O.L. Harbury, E.W. Holmes, Disruption of the purine nucleotide cycle by inhibition of adenylosuccinate lyase produces skeletal

muscle dysfunction, J. Clin. Investig. 74 (1984) 1422–1427 https://doi: 10.1172/JCI111553.
[41] M.-J. MacDonald, Metabolism of the insulin secretagogue methylsuccinate by pancreatic islets, Arch. Biochem. Biophys. 300 (1993) 201–205, https://doi.org/10.1006/abbi.1993.1028.
[42] W.J. Malaisse, A. Sener, Metabolic effects and fate of succinate esters in pancreatic islets, Am. J. Physiol. 264 (1993) E434–E440 https://doi: 10.1152/ajpendo.1993.264.3.E434.
[43] D.C. Chan, Mitochondria: dynamic organelles in disease, aging, and development, Cell 125 (2006) 1241–1252 https://doi: 10.1016/j.cell.2006.06.010.
[44] H. Li, Z. Tang, P. Chu, Y. Song, Y. Yang, B. Sun, M. Niu, E. Qaed, A. Shopit, G. Han, X. Ma, J. Peng, M. Hu, Z. Tang, Neuroprotective effect of phosphocreatine on oxidative stress and mitochondrial dysfunction induced apoptosis in vitro and in vivo: involvement of dual PI3K/Akt and Nrf2/HO-1 pathways, Free Radic. Biol. Med. 120 (2018) 228–238, https://doi.org/10.1016/j.freeradbiomed.2018.03.014.
[45] S. Kovac, A.T. Dinkova Kostova, A.M. Herrmann, N. Melzer, S.G. Meuth, A. Gorji, Metabolic and homeostatic changes in seizures and acquired epilepsy-mitochondria, calcium dynamics and reactive oxygen species, Int. J. Mol. Sci. 18 (2017) 9, https://doi.org/10.3390/ijms18091935.
[46] C.A. Reid, S. Mullen, T.H. Kim, S. Petrou, Epilepsy, energy deficiency and new therapeutic approaches including diet, Pharmacol. Ther. 144 (2014) 192–201 https://doi:10.1016/j.pharmthera.2014.06.001.
[47] S. Rowley, M. Patel, Mitochondrial involvement and oxidative stress in temporal lobe epilepsy, Free Radic. Biol. Med. 62 (2013) 121–131, https://doi.org/10.1016/j.freeradbiomed.2013.02.002.
[48] S. Kovac, A.M. Domijan, M.C. Walker, A.Y. Abramov, Prolonged seizure activity impairs mitochondrial bioenergetics and induces cell death, J. Cell Sci. 125 (2012) 1796–1806 https://doi: 10.1242/jcs.099176.
[49] K. Ryan, D.S. Backos, P. Reigan, M. Patel, Post-translational oxidative modification and inactivation of mitochondrial complex I in epileptogenesis, J. Neurosci. 32 (2012) 11250–11258, https://doi.org/10.1523/JNEUROSCI.0907-12.2012.
[50] L.P. Liang, Y.S. Ho, M. Patel, Mitochondrial superoxide production in kainate-induced hippocampal damage, Neuroscience 101 (2000) 563–570, https://doi.org/10.1016/S0306-4522(00)00397-3.
[51] S.G. Jarrett, L.P. Liang, J.L. Hellier, K.J. Staley, M. Patel, Mitochondrial DNA damage and impaired base excision repair during epileptogenesis, Neurobiol. Dis. 30 (2008) 130–138, https://doi.org/10.1016/j.nbd.2007.12.009.
[52] S. Waldbaum, L.P. Liang, M. Patel, Persistent impairment of mitochondrial and tissue redox status during lithium-pilocarpine-induced epileptogenesis, J. Neurochem. 115 (2010) 1172–1182, https://doi.org/10.1111/j.1471-4159.2010.07013.x.
[53] X. Zhu, J. Dong, B. Han, R. Huang, A. Zhang, Z. Xia, H. Chang, J. Chao, H. Yao, Neuronal nitric oxide synthase contributes to PTZ kindling-induced cognitive impairment and depressive-like behavior, Front. Behav. Neurosci. 11 (2017) 203, https://doi.org/10.3389/fnbeh.2017.00203.
[54] T. Shekh-Ahmad, A. Lieb, S. Kovac, L. Gola, W. Christian Wigley, A.Y. Abramov, M.C. Walker, Combination antioxidant therapy prevents epileptogenesis and modifies chronic epilepsy, Redox Biol. 26 (2019), https://doi.org/10.1016/j.redox.2019.101278 101278.
[55] S. Kovac, A.M. Domijan, M.C. Walker, A.Y. Abramov, Seizure activity results in calcium- and Mitochondria-independent ROS production via NADPH and xanthine oxidase activation, Cell Death Dis. 5 (2014) e1442, , https://doi.org/10.1038/cddis.2014.390.
[56] Y. Ueda, H. Yokoyama, R. Niwa, R. Konaka, H. Ohya-Nishiguchi, H. Kamada, Generation of lipid radicals in the hippocampal extracellular space during kainic acid-induced seizures in rats, Epilepsy Res. 26 (1997) 329–333, https://doi.org/10.1016/S0920-1211(96)00901-1.
[57] H. Baran, K. Vass, H. Lassmann, O. Hornykiewicz, The cyclooxygenase and lipoxygenase inhibitor BW755C protects rats against kainic acid-induced seizures and neurotoxicity, Brain Res. 646 (1994) 201–206, https://doi.org/10.1016/0006-8993(94)90078-7.
[58] H. Yu, T. Kalogeris, R.J. Korthuis, Reactive species-induced microvascular dysfunction in ischemia/reperfusion, Free Radic. Biol. Med. 135 (2019) 182–197, https://doi.org/10.1016/j.freeradbiomed.2019.02.031.
[59] Y.C. Chuang, A.Y. Chang, J.W. Lin, S.P. Hsu, S.H. Chan, Mitochondrial dysfunction and ultrastructural damage in the hippocampus during kainic acid-induced status epilepticus in the rat, Epilepsia 45 (2004) 1202–1209, https://doi.org/10.1111/j.0013-9580.2004.18204.x.
[60] W.S. Kunz, A.P. Kudin, S. Vielhaber, I. Blümcke, W. Zuschratter, J. Schramm, H. Beck, C.E. Elger, Mitochondrial complex I deficiency in the epileptic focus of patients with temporal lobe epilepsy, Ann. Neurol. 48 (2000) 766–773, https://doi.org/10.1002/1531-8249(200011)48:5<766::AID-ANA10>3.0.CO;2-M.
[61] A.P. Kudin, D. Malinska, W.S. Kunz, Biochim. Biophys. Acta 1777 (2008) 689–695.
[62] A. Panov, P. Schonfeld, S. Dikalov, R. Hemendinger, H.L. Bonkovsky, B.R. Brooks, The neuromediator glutamate, through specific substrate interactions, enhances mitochondrial ATP production and reactive oxygen species generation in non-synaptic brain mitochondria, J. Biol. Chem. 284 (2009) 14448–14456, https://doi.org/10.1074/jbc.M900985200.
[63] S.J. Ralph, R. Moreno-Sánchez, J. Neuzil, Inhibitors of succinate: quinone reductase/Complex II regulate production of mitochondrial reactive oxygen species and protect normal cells from ischemic damage but induce specific cancer cell death, Pharm. Res. 28 (2011) 2695–2730, https://doi.org/10.1007/s11095-011-0566-7.
[64] T. Shekh-Ahmad, S. Kovac, A.Y. Abramov, Reactive oxygen species in status epilepticus, Epilepsy Behav. 106410 (2019), https://doi.org/10.1016/j.yebeh.2019.07.011.
[65] D.E. Naylor, H. Liu, C.G. Wasterlain, Trafficking of GABA(A) receptors, loss of inhibition, and a mechanism for pharmacoresistance in status epilepticus, J Neurosci 25 (2005) 7724–7733, https://doi.org/10.1523/JNEUROSCI.4944-04.2005.
[66] J. Kapur, Role of NMDA receptors in the pathophysiology and treatment of status epilepticus, Epilepsia Open 3 (2018) 165–168, https://doi.org/10.1002/epi4.12270.
[67] D.E. Naylor, H. Liu, J. Niquet, C.G. Wasterlain, Rapid surface accumulation of NMDA receptors increases glutamatergic excitation during status epilepticus, Neurobiol. Dis. 54 (2013) 225–238, https://doi.org/10.1016/j.nbd.2012.12.015.
[68] S. Ding, In vivo astrocytic Ca(2+) signaling in health and brain disorders, Future Neurol. 8 (2013) 529–554.
[69] M. Gómez-Gonzalo, G. Losi, A. Chiavegato, M. Zonta, M. Cammarota, M. Brondi, F. Vetri, L. Uva, T. Pozzan, M. de Curtis, G.M. Ratto, An excitatory loop with astrocytes contributes to drive neurons to seizure threshold, PLoS Biol. 8 (2010) e1000352, , https://doi.org/10.1371/journal.pbio.1000352.
[70] G. Carmignoto, P.G. Haydon, Astrocyte calcium signaling and epilepsy, Glia 60 (2012) 1227–1233, https://doi.org/10.1002/glia.22318.
[71] J.E. Kim, T.C. Kang, PKC, AKT and ERK1/2-mediated modulations of PARP1, NF-κB and PEA15 activities distinctly regulate regional specific astroglial responses following status epilepticus, Front. Mol. Neurosci. 12 (2019) 180, https://doi.org/10.3389/fnmol.2019.00180.
[72] Y. Ma, R. Li, Y. Zhang, L. Zhou, Y. Dai, Knockdown of peroxiredoxin 5 inhibits the growth of osteoarthritic chondrocytes via upregulating Wnt/β-catenin signaling, Free Radic. Biol. Med. 76 (2014) 251–260, https://doi.org/10.1016/j.freeradbiomed.2014.08.015.
[73] Y. Xing, W. Bao, X. Fan, K. Liu, X. Li, T. Xi, A novel oxaliplatin derivative,Ht-2,triggers mitochondrion-dependent apoptosis in human colon cancer cells, Apoptosis 20 (2015) 83–91, https://doi.org/10.1007/s10495-014-1044-6.
[74] X. Zhang, D. Liang, X. Lian, Y. Jiang, H. He, W. Liang, Y. Zhao, Z.H. Chi, Berberine activates Nrf2 nuclear translocation and inhibits apoptosis induced by high glucose in renaltubular epithelial cells through a phosphatidylinositol 3-kinase/Akt-dependent mechanism, Apoptosis 21 (2016) 721–736, https://doi.org/10.1007/s10495-016-1234-5.
[75] B. Kalyanaraman, V. Darley-Usmar, K.J. Davies, P.A. Dennery, H.J. Forman, M.B. Grisham, G.E. Mann, K. Moore, L.J. Roberts, H. Ischiropoulos, Measuring reactive oxygen and nitrogen species with fluorescent probes: challenges and limitations, Free Radic. Biol. Med. 52 (2012) 1–6, https://doi.org/10.1016/j.freeradbiomed.2011.09.030.
[76] K. Wang, D.J. Klionsky, Mitochondria removal by autophagy, Autophagy 7 (2011) 297–300, https://doi.org/10.4161/auto.7.3.14502.
[77] Q. Lin, S. Li, N. Jiang, X. Shao, M. Zhang, H. Jin, Z. Zhang, J. Shen, Y. Zhou, W. Zhou, L. Gu, R. Lu, Z. Ni, PINK1-parkin pathway of mitophagy protects against contrast-induced acute kidney injury via decreasing mitochondrial ROS and NLRP3 inflammasome activation, Redox Biol. 26 (2019), https://doi.org/10.1016/j.redox.2019.101254 101254.
[78] M. Wu, X. Liu, X. Chi, L. Zhang, W. Xiong, S.M.V. Chiang, D. Zhou, J. Li, Mitophagy in refractory temporal lobe epilepsy patients with hippocampal sclerosis, Cell. Mol. Neurobiol. 38 (2018) 479–486, https://doi.org/10.1007/s10571-017-0492-2.
[79] Y. Han, Y. Lin, N. Xie, Y. Xue, H. Tao, C. Rui, J. Xu, L. Cao, X. Liu, H. Jiang, Z. Chi, Impaired mitochondrial biogenesis in hippocampi of rats with chronic seizures, Neuroscience 194 (2011) 234–240, https://doi.org/10.1016/j.neuroscience.2011.07.068.
[80] Y. Lin, J. Xu, L. Cao, Y. Han, J. Gao, N. Xie, X. Zhao, H. Jiang, Z. Chi, Mitochondrial base excision repair pathway failed to respond to status epilepticus induced by pilocarpine, Neurosci. Lett. 474 (2010) 22–25, https://doi.org/10.1016/j.neulet.2010.02.065.
[81] Z.H. Sheng, Mitochondrial trafficking and anchoring in neurons: new insight and implications, J. Cell Biol. 204 (2014) 1087–1098, https://doi.org/10.1083/jcb.201312123.
[82] J. Liu, A. Wang, L. Li, Y. Huang, P. Xue, A. Hao, Oxidative stress mediates hippocampal neuron death in rats after lithium pilocarpine-induced status epilepticus, Seizure 19 (2010) 165–172, https://doi.org/10.1016/j.seizure.2010.01.010.
[83] E. Roberts, S. Frankel, gamma-Aminobutyric acid in brain: its formation from glutamic acid, J. Biol. Chem. 187 (1950) 55–63.
[84] N. Bouché, A. Fait, D. Bouchez, S.G. Møller, H. Fromm, Mitochondrial succinic-semialdehyde dehydrogenase of the gamma-aminobutyrate shunt is required to restrict levels of reactive oxygen intermediates in plants, Proc. Natl. Acad. Sci. U. S. A. 100 (2003) 6843–6848, https://doi.org/10.1073/pnas.1037532100.
[85] D.M. Treiman, GABAergic mechanisms in epilepsy, Epilepsia 42 (2001) 8–12, https://doi.org/10.1046/j.1528-1157.2001.042suppl.3008.x 10.1046/j.1528-1157.2001.042suppl.3008.x.
[86] R. Balazs, Y. Machiyama, B.J. Hammond, T. Julian, D. Richter, The operation of the gamma-aminobutyrate bypath of the tricarboxylic acid cycle in brain tissue in vitro, Biochem. J. 116 (1970) 445–461, https://doi.org/10.1042/bj1160445.
[87] W. Yue, Y.X. Liu, D.L. Zang, M. Zhou, F. Zhang, L. Wang, Inhibitory effects of succinic acid on chemical kindling and amygdala electrical kindling in rats, Acta Pharmacol. Sin. 23 (2002) 847–850.
[88] C. Roehrs, E.R. Garrido-Sanabria, A.C. Da Silva, L.C. Faria, V.D. Sinhorin, R.H. Marques, M.R. Priel, M.A. Rubin, E.A. Cavalheiro, Succinate increases neuronal post-synaptic excitatory potentials in vitro and induces convulsive behavior through N-methyl-d-aspartate-mediated mechanisms, Neuroscience 125 (2004) 965–971, https://doi.org/10.1016/j.neuroscience.2004.01.058.
[89] B. Hassel, U. Sonnewald, Selective inhibition of the tricarboxylic acid cycle of GABAergic neurons with 3-nitropropionic acid in vivo, J. Neurochem. 65 (1995) 1184–1191, https://doi.org/10.1046/j.1471-4159.1995.65031184.x.
[90] T. Alexi, P.E. Hughes, R.L.M. Faull, C.E. Williams, 3-Nitropropionic acid's lethal

triplet: cooperative pathways of neurodegeneration, Neuroreport 9 (1998) 57–64.
[91] E.M. Urbanska, P. Blaszczak, T. Saran, Z. Kleinrok, W.A. Turski, Mitochondrial toxin 3-nitropropionic acid evokes seizures in mice, Eur. J. Pharmacol. 359 (1998) 55–58, https://doi.org/10.1016/s0014-2999(98)00648-7 10.1016/S0014-2999(98)00648-7.
[92] L. Hertz, D.L. Rothman, Glucose, lactate, β-hydroxybutyrate, acetate, GABA, and succinate as substrates for synthesis of glutamate and GABA in the glutamine-glutamate/GABA cycle, Adv. Neurobiol. 13 (2016) 9–42, https://doi.org/10.1007/978-3-319-45096-4_2.